Earth and Planetary Science Letters

Embryos of TTGs in Gore Mountain garnet megacrysts from water-fluxed melting of the lower crust

--Manuscript Draft--

Manuscript Number:	EPSL-D-20-01737R1
Article Type:	Letters
Keywords:	TTG; megacrysts; nanogranitoids; crustal melting; garnet; trondhjemite
Corresponding Author:	Silvio Ferrero, Ph.D. Universität Potsdam Potsdam, GERMANY
First Author:	Silvio Ferrero, Ph.D.
Order of Authors:	Silvio Ferrero, Ph.D.
	Iris Wannhoff
	Oscar Laurent
	Chris Yakymchuk
	Robert Darling
	Bernd Wunder
	Alessia Borghini
	Patrick J. O'Brien
Abstract:	The garnet megacrysts of Gore Mountain (Adirondacks, US) are world-renown crystals due to their size, up to 1 m in historical record, which makes them the largest known garnets on the planet. We show here that they are also host to the first primary inclusions of trondhjemitic melt found in natural mafic rocks. The petrological and experimental investigation of the inclusions, coupled with phase equilibrium modelling, shows that this melt is the result of H 2 O-fluxed partial melting at T >900°C of a lower crustal gabbro. The compositional similarity between the trondhjemitic melt inclusions and tonalitic–trondhjemitic–granodioritic (TTGs) melts makes these inclusions a direct natural evidence that melting of mafic rocks generates TTG-like melts, and provide us with the possibility to clarify processes responsible for the formation of the early continental crust. These TTG embryos represent the trondhjemitic end-member of the melts whose emplacement at upper crustal levels, after being modified by mixing and crystallization-related processes, leads to the formation of the TTG terranes. Moreover, our study shows how the melt from H 2 O-fluxed melting of mafic lower crust has mismatched major and trace element signatures, previously interpreted as evidence of melting at very different pressures. This poses serious limitations to the established use of some chemical features to identify the geodynamic settings (e.g. subduction versus thickened crust) responsible for TTG generation and the growth of early crust.

Potsdam, 16/03/2021

Cover letter

Dear Editor,

The present letter accompanies the submission of the revised version of the paper "Embryos of TTGs in Gore Mountain garnet megacrysts from water-fluxed melting of the lower crust" from myself, Wannhoff, Laurent, Yakymchuk, Darling, Wunder, Borghini, O'Brien.

We are grateful to the reviewers for their comments and observations. We accepted most of the suggested changes. We expanded the text and/or simplified it where suggested by reviewer #1 and #2, and inserted appropriate comments and references in keeping with the latest paper on the area from Shinevar et al. 2021, which became accessible 3 weeks ago and support fully our results. We answered each comment in detail (see below).

We modified figure 7 of the original version by adding more diagrams to discuss the data (as suggested by reviewer #1), changing the visualization style of the single data (they are not grouped in clouds any longer) and splitting the figure in 2, which resulted in adding one figure (Fig. 8) to the manuscript. We modified also table 1 to include each single melt analysis and we added a new database (containing the experimental melts used in figures 7 and 8) as supplementary file Table S3, as suggested by reviewer #1. Finally, we modified the colour palette of each figure top meet color-blind friendly standards.

The methods in supplementary file were also slightly modified to clarify the alkali-correction procedure (reviewer #1).

Please let us now if further clarifications are needed.

Best regards

Silvio Ferrero and co-authors

Reviewers' comments:

Reviewer #1: Review of "Embryos of TTGs in Gore Mountain garnet megacrysts from water-fluxed melting of the lower crust" (Ferrero et al.)
By O. Jagoutz

The paper presents a detailed study of melt inclusion hosted in megacrystic garnet from the gore mountain garnet granulite. The paper's key conclusions are 1) the rocks enjoyed much higher temperature than previously assumed and 2) that partial meting is the essential process to produce Archean TTG.
I read the paper with great interest and recommend it for publication after some (major) revision. The paper reads as if it was initially written for a short format journal and subsequent extended for EPSL (as we all often do). However, the paper's style is still more akin to what one expects in short format journals and not appropriate for EPSL. The text should be thoroughly reworked, more nuanced, less speculative, and a more in-depth discussion of the data is essential.

Thanks for the suggestion. The text was already thoroughly expanded to clarify many aspects which were unclear in the shorter version of the paper, and at the same time we tried to keep it synthetic enough to avoid excessive speculations. The new version of the paper submitted along with this letter makes fully use of the 6500 words limit allowed by the EPSL format and make up for the shortcomings pointed out by the reviewer.

In my opinion, the paper should be strengthened along the following recommendations:
1) We recently published a paper in JPet (Shinevar et al., 2021) that comes to the same conclusion as the manuscript concerning the P, T estimates of the gore mountain garnet granulites. So the statement that these are 'surprising' high estimates for UHT conditions in these rocks should be discussed more nuanced and our recent paper more considered when discussing published P, T estimates.

Agree. Although we were aware of the JPet paper in preparation, we had access to the final accepted version only after submitting the present version of the paper. Our revised paper now takes in account the new findings of Shinevar et al. (2021) and cite it/discuss it where appropriate. Also, we removed the “unexpected outcome” part (line 314).

But it is exciting to see that this manuscript corroborates our finding.

Agree!

2) The manuscript tries to make a significant point that the MI's analyzed in grt from Gore mountain granulites are key to understand TTG formation. I have (obviously) some issues with this discussion, as the paper stretches the importance of their finding beyond what I consider reasonable. The authors try to make a point that their finding 'strengthens' the idea that TTG is generally formed in a two-stage

process whereby a basaltic/gabbroic precursor remelted to form TTG because the lower crust is being flushed with H2O and hot. I think this part is where the authors need to be true to the observations: The MI could indeed represent melt inclusions, but there is no evidence that these rocks lost any significant melt.

We see the point the reviewer is making, but we would like to stress that whether these rocks lost melt is irrelevant for the purpose of the paper. What we discuss in the manuscript is the mechanism of mafic melting producing a trondhjemitic melt, not the generation of TTG bodies in this particular area (this is discussed in greater details in the answer to the next part of the comment below). We have a protolith that has melted and still preserve melt as inclusions, and this allow us to draw some new considerations on the petrogenesis of this type of melts. We are very clear in pointing out the differences between these TTG embryos and "real" TTGs in paragraph 4.4 and 4.5 (now 4.5 and 4.6 respectively), and in fact this is the reason why we use the terminology TTG embryos rather than simply TTGs or nanoTTGs, discussing this choice at length in paragraph 4.4 (now 4.5).

The 'white' stuff shown in figure 6 is not a melt (as alluded to in the text), and the bulk composition of the garnet granulites is identical to the composition of the protolith (see Shinevar et al. 2021 or other previous studies that all conclude the same). So while the rocks might have locally melted, they have not lost any significant amount of melt to higher crustal levels.

What evidence has the reviewer to rule out so strongly the possibility of the "white stuff" being (at least originally) a melt? As far as we know nobody besides Hollocher (2008) discussed its nature, so we do believe its nature still needs to be clarified, as it is the only portion of the garnet amphibolites that indeed may look like a crystallized melt of some sort (see lines 271-298). On another note, we totally agree with what Shinevar et al. (as well as previous authors) states in the paper, e.g. that the amphibolites did not change composition with respect to the gabbro (with the exception of water). We added lines 295-298 to make this clear.

So they are NOT the source regions for TTG's. Additionally, it's important to keep in mind that these garnet granulites crop out in a tiny area related to a specific structural situation (next to a fault zone), and it is quite a stretch, in my opinion, to cite the finding of these unusual rocks as representative for key processes in the lower crust. It is generally concluded, as does this manuscript, that the fault zone along which these rocks outcrop, was a pathway for the fluid that interacted with and formed these grt granulites. We don't know if fluids flush the entire lower crust to form large batholiths of TTG.

As it is clear from the comment of the reviewer, our original text clearly misled the reader about what is the main target of this manuscript. We modified significantly the introduction to improve clarity on this point (lines 77-83). We would like to clarify however that nowhere in the manuscript we say that this particular case of melting of this gabbro generated bodies of TTGs. What this case (indisputably, in our view) does is offering a completely new glimpse into the mechanisms of mafic melting, both how it may proceed (e.g. involving water) and what are the products of this process. Melt composition is consistent with mafic melting and close to TTG like

magmas, and lower crustal rocks of mafic composition have been proposed as possible sources of TTGs. So even if exactly those rocks did not generate TTG bodies, the mechanism operating there (mafic melting of lower crustal rocks producing a trondhjemite) are the same many authors have proposed to take place where TTGs are generated.

There are multiple ways to form TTG, and both likely occur in nature. Indeed there are vast outcrops of lower crustal magmatic cumulates complementary to TTG granitoid those cant be dismissed based on the presented manuscript. Additionally, multiple experimental studies provide strong evidence that hydrous fractional crystallization could be a key process to form TTG. As the Italians say: Many roads lead to Rom….

We absolutely agree that it is not possible to propose a “one size fits all” type of model for TTG generation. What we propose is that our finding support one model in particular, but this does not mean at all that our findings invalidate all the other models. We modified the conclusions (lines 554-558) to clarify how our finding does not pose any problem to the existence of other mechanisms of TTG production.

3) Instead of the more speculative discussion/conclusions, I would like to see a more in-depth discussion of the analytical data. I was surprised to read that glass is still preserved in these inclusions that formed 1 Ga ago and cooled very, very slowly in the lower crust. That observation needs to be discussed in much greater detail.

Agree. The presence of glass is rather common in nanogranitoids, and its presence is closely related to presence of polymorphs, and for this reason it will be discussed along with such phases (see answer to comment number 5).

Even more so, as the glass composition is much more akin to a granitic minimum melt than the bulk re-integrated MI compositions (which are more Na-rich).

As stated at line 141-143, this melt is residual after crystallization of some phases inside the same inclusion, so it is expected to be different from the fully re-homogenized inclusions. Its similarity with the minimum granitic melt is entirely coincidental.

The supplement hints at significant alkali loss during analyses (16-24% relative to Na) but not the main text. How is the alkali loss quantified, was it corrected, and how much did that change the results? The paper addresses these issues neither in the main text nor in the supplement. Table S2 refers to a "High resolution investigation and microchemistry" section that I have not been able to find.

The procedure is already clearly described in the supplementary material. The section “High resolution investigation and microchemistry” is the first one of the files, with the alkali correction procedure explained in the first page. To avoid confusions, we reworded this part of the text to provide more details on the procedure we followed. To clarify matters for the reader we also added some words at line 167-168 in the main text.

4) Experimental work shows clearly that high Na/K melts only form from high Na/K precursors (see e.g. Jagoutz, 2012 for a compilation of experiments). I tried to eyeball the melt composition and the bulk rock composition, and it looks like it fits this general trend. But in general, the melt composition needs to be discussed in more detail. In that respect Figure 7 is not very helpful. Figure 7 a, b, for example, show the same Na-K-Ca systematics (either as element or mineral modes). A classical TAS diagram would be a good start, followed by Harker diagrams etc, that show all reintegrated MI and glass compositions. A detailed comparison between the observed and experimental data would be helpful. Currently, all the manuscript presents are a bunch of colored fields in triangle plots. All data needs to be provided as a table, including the original analysis and the composition corrected for alkali loss.

The text has been modified to discuss more in detail the data (lines 437-446). Figure 7 has been modified adding a TAS diagram and Na_2O vs CaO and Al_2O_3 vs SiO_2 diagrams. Previous figures 7c, d, e,f have been used to create a new figure 8. Table 1 has been also modified and now it contains also each single analysis performed on the re-homogenised inclusions. Table S1 has been then removed because redundant. A table with all the experimental compositions used in figure 7 (and now 8) is now provided as supp material "Table S3_H_2O-present melting experiments from literature".

About the suggestion to add the uncorrected analyses: we believe this is not necessary (indeed this is never done in manuscripts about nanogranitoid studies) because It is well known that analyses of alkali-rich glasses are not representative of the real glass present after the experiment BEFORE the alkali correction is applied. We modified the supplementary material to provide more info on the correction procedure (see answer to point 3) and we believe this is sufficient to clarify this point. If the reviewer is interested in the original analyses I am happy to provide them in a separate email, but adding more analyses to this manuscript would only clog it with unnecessary data.

5) The fact that cristobalite, trilobite, and kumdykolite is present should equally be discussed in detail. What is the explanation for a low P, high T phase like cristobalite or tridymite present in MI that formed at ~ 1 GPa ? Is the kumdykolite a high P or high T phase? Why is its structure preserved if the rocks cooled slowly?

Cristobalite, kumdykolite and glass represent indeed still a quite enigmatic finding. The text has been modified to include more information on them (new paragraph 4.2).

In conclusion, this is a fascinating study that I would like to see published. But its present form has too many loose ends. A thorough major revision is necessary to bring this paper to the EPSL standard.

Hope it helps, Oli.

Reviewer #2: *I reviewed this paper for Geology and liked it then. The authors overstate several aspects of the study, which should be toned down.*

This has been done in the present version of the manuscript, also as reaction to the comments of reviewer #1 (see answer to comment #2 above)

I'd also like to see an expanded discussion of the Laurent NG paper. Please seem my review attachment. Otherwise this is a nice cpntribution that fits well into the EPSL remit.

Detailed review

I reviewed an earlier version of this paper for another journal. I enjoyed reading it then, and I think it has got better with the additional space permitted by EPSL. The study clearly identifies the presence of primary trondhjemitic melt inclusions within garnet porphyroblasts from a the classic Gore Mountain metagabbros, which the authors argue formed by H2O-fluxed melting and that the compositional heterogeneities the melt inclusions preserve questions the validity of using such compositional data for pressure (and depth) estimates. This is an interesting and important finding that chimes with several other recent papers. What I find frustrating is that I am having to make much the same comments as I made in the earlier review. A point I made in the previous review, and repeat, is that the authors claim that their melt inclusions represent "…the first direct natural evidence that melting of mafic rocks generates TTG-like melts…" This is still not true. For example, see Johnson et al. 2012 (Archaean intracrustal differentiation from partial melting of metagabbro—field and geochemical evidence from the central region of the Lewisian complex, NW Scotland, Journal of Petrology 53 (10),2115–2138).

We modified abstract and conclusions and inserted the citation to Johnson et al., (2012). See Lines 560-561.

Statements such as "…they contain trondhjemitic melt inclusions in a mafic source rock, a feature never recognized in previous studies on MI in metamorphic rocks" are obviously fine. Some primary references to TTG magmas should be provided, which were not discovered by Moyen and/or Martin. Perhaps Barker and Arth (1976) deserves a mention (Generation of trondhjemitic tonalitic liquids and Archean bimodal trondhjemite-basalt suites. Geology 4, 596-600).

Unfortunately, the limit of 50 references really makes it difficult to report old literature (even if we agree it is fundamental literature!). We changed the first citation of Moyen and Martin at line 58-59 to "(see Moyen and Martin, 2012 and references therein for a thorough review on the subject)"

As I said earlier, on line 59, "The formation and stabilization of the earliest continental crust are key aspects of planetary evolution" implies that other planets have significant volumes of felsic continental crust. Which planets are these, in which understanding TTGs is so important?

We were referring to the Earth, not other planets. The text has been modified (lines 60-61).

Without wishing to be provocative, I am confused by some aspects on the Laurent et al NG paper. Using their supp. data, if you plot Eu anomaly for their trondhjemites (the supposed plagioclase-rich cumulates) and the felsic volcanic rocks (the supposed evolved melts following plagioclase fractionation) they are indistinguishable (see below). How does this work? In addition, if this model were more generally applicable, where are all the felsic volcanic rocks in greenstone belts to complement the vast volumes of TTGs in Archean lower crustal sections worldwide?

We believe that the present paper is not the right place to defend another (published) paper. In particular, the reviewer made the same comment on a submitted version of a follow-up article to the Laurent et al. NG story, and the revised version of this article (which is to be submitted soon, as I am told by O.Laurent) will certainly be a much more appropriate venue to answer this comment.

I am not suggesting that fractional crystallisation plays a no role in TTG genesis, but I see little evidence that it is significant. Given the weight that is placed on the Laurent et al. paper in the discussion, I do think the reader needs some explanation of these factors

We think that the "weight" given to the Laurent et al NG model in our paper is not as strong as the reviewer suggests - some points of discussion indeed converge, notably the non-uniqueness of the interpretation of trace element signatures in terms of melting pressure, but the overall general model is quite different and the two stories do not depend on each other to be valid. For instance, in the present manuscript we make the case that trondhjemitic melts can form directly by partial melting of mafic rocks, whereas the Laurent et al. model argue that trondhjemites are simply not melts but cumulates instead. In short, the story of the present paper is just not the same as the one defended in the Laurent et al. paper.

Embryos of TTGs in Gore Mountain garnet megacrysts from water-fluxed melting of the lower crust

S. Ferrero[1,2], I. Wannhoff[3], O. Laurent[4,5], C. Yakymchuk[6], R. Darling[7], B. Wunder[8], A. Borghini[1] and P. O´Brien[1].

[1]*Universität Potsdam, 14476 Potsdam-Golm, Germany; sferrero@uni-potsdam.de; borghini@uni-potsdam.de; obrien@uni-potsdam.de*

[2] *Museum für Naturkunde (MfN), 10115 Berlin, Germany;*

[3] *Freie Universität Berlin, 12249 Berlin, Germany; iris.wannhoff@fu-berlin.de*

[4]*ETH, Zurich, Department Erdwissenschaften, Institute for Mineralogy and Petrology, 8092 Zürich, Switzerland*

[5]*CNRS, Observatoire Midi-Pyrénées, Géosciences Environnement, 31400 Toulouse, France; oscar.laurent@Get.omp.eu*

[6]*University of Waterloo, Waterloo, ON N2L 3G1, Canada; chris.yakymchuk@uwaterloo.ca*

[7] *SUNY College at Cortland, NY 13045,US; robert.darling@cortland.edu*

[8]*GFZ, German Research Centre for Geosciences, 14473 Potsdam, Germany; wunder@gfz-potsdam.de*

Abstract

The garnet megacrysts of Gore Mountain (Adirondacks, US) are world-renown crystals due to their size, up to 1 m in historical record, which makes them the largest known

garnets on the planet. We show here that they are also host to the first primary inclusions of trondhjemitic melt found in natural mafic rocks. The petrological and experimental investigation of the inclusions, coupled with phase equilibrium modelling, shows that this melt is the result of H_2O-fluxed partial melting at T > 900 °C of a lower crustal gabbro. The compositional similarity between the trondhjemitic melt inclusions and tonalitic–trondhjemitic–granodioritic (TTGs) melts makes these inclusions a ~~the first~~ direct natural evidence that melting of mafic rocks generates TTG-like melts, and provide us with the possibility to clarify processes responsible for the formation of the early continental crust. These TTG embryos represent the trondhjemitic end-member of the melts whose emplacement at upper crustal levels, after being modified by mixing and crystallization-related processes, leads to the formation of the TTG terranes. ~~Moreover~~Moreover, our study shows how the melt from H_2O-fluxed melting of mafic lower crust has mismatched major and trace element signatures, previously interpreted as evidence of melting at very different pressures. This poses serious limitations to the established use of some chemical features to identify the geodynamic settings (e.g. subduction versus thickened crust) responsible for TTG generation and the growth of early crust.

1. Introduction

The garnet megacrysts of Barton mine, Gore Mountain (Adirondack Highlands, USA) are world-renowned both among petrologists and collectors for their exceptional size - 1 m crystals are recorded historically, making them some of the largest known garnets on the planet, and for their industrial use as abrasive material, with mining having occurred continuously from 1878 to 1983 (Kelly and Darling, 2008). These specimens

also display another crucial feature: the presence of silicate melt preserved as crystallized and glass-bearing inclusions of primary nature. Garnet is one of the most common and widely stable peritectic phases in metamorphic crustal rocks (Baxter et al., 2013), and it has been proven to be able to trap and preserve the melt resulting from crustal melting in more than 40 localities worldwide (Nicoli and Ferrero, ~~under review~~accepted; Ferrero et al., 2018). Although melt inclusions (MI) are being increasingly recognized as a common feature of ~~high grade~~high-grade terranes (Bartoli and Cesare, 2020), the Gore Mountain inclusions are unique because they contain trondhjemitic melt inclusions in a mafic source rock, a feature never ~~recognized~~ reported in previous studies on MI in metamorphic rocks.

Partial melting of a mafic sources has been invoked for the formation of the tonalite, trondhjemite and granodiorite (TTG) rocks, suites of sodium-rich, potassium-poor granitoids, which form the bulk of early Earth´s preserved crust (see Moyen and Martin, 2012 and references therein for a thorough review on the subject). The formation and stabilization of the earliest continental crust are key aspects of planetary evolution that can create conditions suitable for the development of complex life. Constraining the origin of TTGs is, therefore, important for models of early ~~planetary~~ evolution of our planet.

Although the source rocks of TTGs are commonly inferred to be hydrated mafic rocks (Moyen and Martin, 2012), there are no known examples of melt inclusions in garnet in such metabasites. TTGs have been proposed to be generated by partial melting of subducted mafic rocks at very high pressures (HP, >2.5 GPa, Moyen, 2011) or at much shallower lower crustal conditions (<1.5 GPa) via amphibole-breakdown (Johnson et al., 2013, 2017) or water-fluxed melting (Pourteau et al., 2020). Other models propose that TTG magmas result from fractional crystallization of intermediate-mafic magmas (Jagoutz

et al., 2013; Smithies et al., 2019) possibly associated with crystal-liquid unmixing in shallow magma chambers feeding silicic eruptions (Laurent et al., 2020). The formation mechanisms of the parental TTG magmas at lower crustal depths have been investigated via geochemical and petrological characterization of TTG rocks emplaced at shallower levels (e.g. Moyen and Martin, 2012), forward modelling of putative analogues for source rocks exposed in Archean terranes (Johnson et al., 2017; Smithies et al., 2019), or using experiments (e.g. Laurie and Stevens, 2012; Qian and Hermann, 2013) and thermodynamic modelling (e.g. Kendrick and Yakymchuk, 2020).

Our finding provides a novel tool, i.e., the study of preserved MI in ~~high grade~~ high-grade rocks, for the investigation of melting mechanisms in a natural mafic source region. More importantly, despite the fact that the target rocks are not Archean in age and TTG bodies are absent in the area, the similarities between the targeted MI and the TTG magmas both in terms of composition and genetic process makes of the present case study the missing link between nature, experiments and modelling results on the model of TTG petrogenesis via mafic melting. ~~Direct observations from a preserved natural source region are therefore essential to validate one of the models and thus constrain the depth of TTG magma production. Our finding provides the missing link between nature and the results of experiments and modelling, offering the possibility to investigate TTG formation processes using the powerful tool represented by MI studies in partially melted, high grade rocks.~~

2. Sample description

The rock investigated in this study is a garnet amphibolite of Mesoproterozoic age sampled in the pit 1 of the currently inactive mining site of Barton Mine, now Garnet Mine Tours in the Adirondacks (43°40'56"N, 74°2'51"W, Fig. 1a,b), which is an outlier of the Grenvillian orogeny (Rivers, 1997). The most apparent feature of the investigated rocks is the presence of garnet megacrysts. They form large porphyroblasts, subhedral to euhedral in shape (Fig. 1c), with size visible at the present day in the outcrop of ≤35 cm in diameter (Kelly and Darling, 2008). Despite their size, the garnet porphyroblasts show a remarkably homogenous composition with high almandine and pyrope components and minor grossular ($Alm_{44}Prp_{42}Grs_{14}Sps_{1}$, Supplementary table S1; for details on analytical methods and techniques see the Supplementary Material). Almost every garnet is entirely surrounded by a shell of coarse-grained idiomorphic hornblende, several cm-wide (Fig. 1c). The crystallographic faces of garnet appear generally preserved at the garnet–hornblende interface at the outcrop and hand sample scale. Locally however garnet can also be surrounded by sub-millimetric ~~-scale~~ symplectitic rims containing fine-grained hornblende, plagioclase, orthopyroxene and minor biotite, that formed during retrogression (mineral compositions are in Supplementary table S1; see also Hollocher, 2008). Garnet porphyroblasts and hornblende shells are hosted in a granoblastic matrix composed mainly of plagioclase and hornblende (the latter identical in major element compositions to the shell hornblende; Supplementary Table S1), plagioclase and orthopyroxene (Fig. 1c), with minor biotite and pyrite.

Previous authors generally agree that these amphibolites are the result of high-grade metamorphism during the collapse of the Ottawan orogen at 1050 Ma (e.g. McLelland and Selleck, 2011). The protolith is an olivine-bearing gabbro exposed

adjacent to the amphibolites (Fig. 1b) and was originally emplaced at ~1150 Ma as part of an anorthosite-mangerite-charnockite-granite (AMCG) suite in the basement of the Adirondacks (Fig. 1a; Rivers, 1997). The extreme grain size of the rock, especially of the garnet porphyroblasts, coupled with the abundance of amphibole with respect to the gabbro protolith, has prompted several authors to ~~infer~~ propose the flux of a "copious amount of fluid" during metamorphism (McLelland and Selleck, 2011). This likely occurred along a shear zone at the contact between gabbro and syenite (Fig. 1b), inferred to be a preferential pathway for fluid ingress (Goldblum and Hill, 1992).

3. Results

3.1 Crystallized melt inclusions

The garnet megacrysts contain a relatively large amount of polycrystalline inclusions along with crystallographically-oriented rutile needles (Fig. 2a, b). Polycrystalline inclusions are distributed as clusters in the inner portion of the garnet, which is unequivocal evidence of ~~trapping~~ entrapment during garnet growth (Ferrero et al., 2018 and references therein); these inclusions are therefore primary in nature. The inclusions are aggregates of micrometric crystals in cavities of mostly isometric shape with size ≤ 50 µm across, with the smallest inclusions (<15 µm) displaying negative crystal shapes (i.e. mimicking the shape of the host garnet; Fig. 2b, c, d, e). Many inclusions have elongated tubular shapes with lengths of ≤150 µm and diameters of ≤10 µm (Fig. 1b), parallel to rutile needles. Decrepitation cracks ~~(e.g. Ferrero et al., 2016)~~ are generally absent in the inclusions regardless their shape.

A combination of Raman spectroscopy and Field Emission Gun (FEG) electron probe microanalysis (EPMA) has shown that most of the inclusions contain an assemblage consisting of cristobalite (Fig. 2e, f; already identified by Darling et al., 1997), quartz or ~~trydimite~~tridymite, plus kumdykolite (an albite polymorph; Ferrero et al., 2016) and one or both of the OH-bearing phases anthophyllite and pargasite (Fig. 2c, d, e, f). Minor amounts of phlogopite and osumilite are also present. Orthopyroxene, apatite, ilmenite and rutile needles may occur in the MI and are interpreted as trapped accessory phases, as they are also present as mineral inclusions in the host garnet. The association of polymorphs of silica and feldspars plus OH-bearing phases is characteristic of nanogranitoids, i.e., crystallized MI in metamorphic rocks (e.g. Bartoli et al., 2016; Ferrero et al., 2018). One inclusion contains glass along with pargasite and accessory minerals; the glass is probably residual after partial crystallization of the melt originally trapped in the inclusion (Fig. 2f, g; see also glass composition in table 1). Cristobalite is present both as a crystallization product in the nanogranitoids and in association with rutile or ilmenite in a second type of polycrystalline inclusions, whose overall composition is incompatible with a former melt nature and thus will not be investigated further.

3.2 Experimental re-homogenization and melt chemistry

Multiple re-heating experiments in the temperature (T) range 900–950°C under confining pressure (P) of 1.0–1.5 GPa were performed using a piston cylinder press to re-homogenize the crystallized inclusions to glass, following the method devised by Bartoli et al. (2013; see also ~~methods in~~ Supplementary Material). Experimental parameters and observations on the products of each run are listed in Fig. 3a. After the

run at 900°C (experiment GM3), the inclusions show no evidence of re-melting, i.e. glass is absent. At 925°C (GM5) only the smallest inclusions (<2 µm) appear to be completely re-homogenized, whereas most inclusions contain glass in association with daughter phases such as kumdykolite and / or amphibole, and were therefore interpreted as having only undergone partial re-melting. Complete re-homogenization of the inclusions is instead common after re-heating at temperature (T) = 940°C (GM7, GM8, GM9), where nanogranitoids turn into a homogenous hydrous glass (Fig. 3b) often containing trapped phases such as orthopyroxene (Fig. 3c), cristobalite, rutile and more rarely ilmenite (~~details on each analyses are in Table S2~~Table 1). At 950°C (GM1) the nanogranitoids are again completely re-homogenized, but cracks are common in the host and locally melt and garnet interact, which indicates disequilibrium between melt and host (Ferrero et al., 2018) and suggests that 950°C is higher than the original entrapment T of the inclusions (see discussion).

The fully re-homogenized inclusions from the experiments at 940°C were analyzed via EPMA on 7 inclusions (Fig., 4a; ~~Supplementary Table S2~~Table1). The resulting glass, after alkali-loss correction (see details on the procedure in Supplementary Material), is a trondhjemite with average SiO_2 = 71.89 wt%; Na_2O/CaO = 2.54 and K_2O/Na_2O ≈ 0.20, low magnesium number (Mg# = [molar $Mg/(Mg+Fe^{2+}_{tot})$] = 0.39) and peraluminous character [Aluminium Saturation Index (ASI) = Al/(Ca+Na+K) = 1.34] ~~(Table 1)~~. The H_2O content, measured by EMP difference, is around 4.28 wt%.

The trace element content of isometric nanogranitoids located below the surface was measured via Laser Ablation Inductively Coupled Plasma Mass Spectrometry (LA-ICP-MS) and the contribution of the host garnet subtracted after the analytical session

(see methods in Supplementary Material; the whole trace element dataset is visible ~~Supplementary~~ Table ~~S3~~S2). Elements enriched in the host (e.g. Y, Heavy Rare Earths Elements - HREE) with respect to the inclusions are not quantifiable with this method due to the dominant signal from the host (Ferrero et al., 2018). The polycrystalline inclusions show strong enrichment in some High Field Strength Elements (HFSE), like Zr, Hf and Ti compared to the protolith gabbro (Fig. 4b), as well as enrichments of Pb, U, Th, Zn and Rare Earths elements (REE) from La to Gd (Fig. 4c). Both melt and gabbro show on average a similar positive Eu anomaly (Fig. 4c).

3.3 Phase equilibrium modelling

Phase equilibrium modelling was used to constrain independently the pressure-temperature (*PT)* conditions of partial melting and peak metamorphism, as well as quantify the concentration of H_2O in the system required to generate the observed mineral assemblage in the garnet amphibolites of Gore Mountain. A key assumption of this modelling approach is the achievement of chemical equilibrium in the system (Lanari and Duesterhoeft, 2019); the macroscopic spatial distribution of garnet at the outcrop scale at Gore Mountain is heterogeneous and the diffusive length scale required to maintain chemical equilibrium between garnet and its matrix is unclear. Keeping this limitation in mind, we use phase equilibrium modelling to provide a first-order assessment of the *P*–*T*–composition *(X)* conditions required for development of the observed mineral assemblages and this approach independently complements other estimates of peak metamorphic conditions, such as melt re-homogenization temperatures (this study) and

trace element thermometry of accessory minerals (Shinevar et al., ~~2020~~2021). The detailed modelling methods are presented in the supplementary material.

A temperature–composition (H_2O) phase diagram was calculated at 1.0 GPa for the inferred protolith (olivine gabbro) over a range of H_2O concentrations—ranging from essentially dry to H_2O-saturated at the wet solidus—to constrain the stability of the peak metamorphic assemblage (garnet, hornblende, orthopyroxene, plagioclase and melt). Orthopyroxene in equilibrium with anatectic melt is predicted to be stable at >~~800ºC~~ 800°C (Fig. 5a), which is a lower limit on the peak temperature. The absence of quartz from inferred peak assemblage further restricts temperatures to > ~~850ºC~~ 850°C (Fig. 5a). The modelled concentration of H_2O in the system during the metamorphic peak (at 1.0 GPa) is restricted to < 4 ~~wt.%~~wt% by the presence of plagioclase and to > 1 ~~wt.%~~wt% H_2O by the solidus at ~~850ºC~~ 850°C (Fig. 5a). An additional constraint on the temperature and H_2O content of the system at peak metamorphism is provided by comparing the observed proportion of garnet in the garnet amphibolites (~13 vol.%; McLelland and Selleck, 2011) with the modelled amount (calculated as mol.% in the modelling, which is roughly equivalent to vol.% on a one-oxide molecular basis). In general, using mineral proportions is considered preferable to using mineral compositions to constrain peak *P*–*T* conditions in high-temperature metamorphic rocks (e.g. White et al., 2011). Using this approach, a modelled 13 mol.% of garnet in the system is restricted to > ~~870ºC~~ 870°C and compositions with ~3 ~~wt.%~~wt% H_2O (Fig. 5a). This indicates that the inferred peak assemblage requires substantial H_2O influx into the system when compared with the composition of the inferred protolith (~0.44 wt% H_2O, McLelland and Selleck, 2011). The temperatures of > ~~900ºC~~ 900°C at 1.0 GPa in the model yield the observed proportion of

garnet (Fig. 5a). Note that the modelled phase assemblage field that contains the observed amount of garnet is also predicted to contain a minor amount of clinopyroxene (< 8 mol.% at 1.0 GPa), which is absent from the Gore Mountain garnet amphibolites. The significance of clinopyroxene to the modelling results is discussed below.

Using the estimated 3 ~~wt.%~~wt% H_2O in the system at the metamorphic peak (Fig. 5a) a pressure–temperature phase diagram was calculated to further constrain the metamorphic peak (Fig. 5b). The inferred peak metamorphic assemblage for the Gore Mountain garnet amphibolites is restricted to a small field at 810–~~890ºC~~ 890°C and 0.9–1.0 GPa. However, the maximum molar proportion of garnet in this field is 7 mol.%, which is roughly half of the observed amount. To achieve a modeled 13 mol.%, garnet requires a predicted mineral assemblage with a minor amount of clinopyroxene (Fig. 5b). The modelled stability of clinopyroxene in anatectic metabasites is usually overestimated by current phase equilibrium modelling techniques. This reflects a limitation of the modelling in which the partitioning of Ca (and some other cations) between amphibole and clinopyroxene does not reproduce natural parageneses accurately (Forshaw et al., 2019). Therefore, this limitation will influence amphibole-rich rocks such as the Gore Mountain garnet amphibolites. Considering this model limitation, if we permit a small amount (< 8 mol.%) of model clinopyroxene into the peak assemblage for the investigated rocks, then the estimated peak *P–T* conditions are restricted to ~1.0 GPa (based on the 13 mol.% garnet isopleth) and to temperatures 850–~~950ºC~~950°C. Along the 13 mol.% garnet isopleth (Fig. 5b), the modeled amount of clinopyroxene decreases from ~8 mol.% at ~~950ºC~~ 950°C to ~2 mol.% at ~~850ºC~~ 850°C (Supplementary Fig. S1d). Therefore, we consider temperatures of > ~~900ºC~~ 900°C permissible by the phase equilibrium modelling,

with the caveat that the stability of clinopyroxene is a source of uncertainty in modelling partial melting of amphibole-rich rocks. These modelled temperatures are consistent with the temperature of MI re-homogenization (900–950°C) and yield a predicted 20–25 mol.% melt (Supplementary Fig. S1a).

4. Discussion

4.1 Silicate melt at Barton mine

Polycrystalline inclusions are present in the garnet megacrysts of Barton mine at Gore Mountain. Their phase assemblages and successful re-homogenization via experimental re-heating, coupled with the presence of preserved glass in one inclusion, demonstrate that such inclusions were originally droplets of melt, now partially to totally crystallized to nanogranitoids. Due to their overall trondhjemitic composition, such inclusions will be hence forward called “nanotrondhjemites” in keeping with the common use in nanogranitoid nomenclature (~~Ferrero et al., 2016;~~ Bartoli and Cesare, 2020). A melt origin for the cristobalite-bearing polycrystalline inclusions in the garnet megacrysts was already proposed by Darling et al. (1997), but no melt compositions were retrieved to support this hypothesis at the time. More recently, Shinevar et al. (2021) proposed the production of a limited amount of melt during the formation of garnet megacrysts at Barton Mine. Moreover, i~~I~~n the Adirondack Highlands~~,~~ nanogranitoids were previously reported in the metapelitic gneisses of Port Leyden (Darling, 2013). ~~More recently,~~ p~~P~~reliminary investigations also show~~ed~~ their presence also in garnets from Hooper mine (Ferrero,

unpublished data), a garnet mine active until 1928 (Darling, pers.comm.), suggesting that partial melting in the area may be more common than previously thought.

~~The crystallization products of the Gore Mountain nanotrondhjemites often include metastable polymorphs such as cristobalite, trydimite and kumdykolite (Ferrero et al., 2016). As such phases are known to revert to their most common counterparts (quartz and albite) in case of inclusion reopening via decrepitation (Ferrero et al., 2016), their presence is regarded as a strong evidence that the MI preserve the composition of the original melt, as already proposed for previous nanogranitoid studies (Bartoli and Cesare, 2020).~~

Although the finding of glass-bearing nanogranitoids ~~makes~~ is a compelling evidence for the (former) presence of melt in the garnet megacrysts ~~undisputable~~, clear leucosome domains are not conspicuous at the outcrop scale. ~~However l~~Leucocratic pockets, several cm across in size, are anyway often visible in pit 1 (Fig. 6a, b). They are mainly composed of coarse-grained plagioclase ± orthopyroxene, and always closely associated with the garnet megacrysts. Commonly these pockets are entirely enclosed within the amphibole shell surrounding the megacrysts, making their formation likely associated to both garnet and amphibole growth (Fig. 6). Such pockets could either be breakdown products of garnet with contribution from the amphibole, or represent crystallized melt. The first possibility can be excluded because the retrograde reaction between garnet and amphibole in these rocks generates submillimetric symplectites of plagioclase + orthopyroxene + hornblende + biotite (Hollocher, 2008), very different both in grain size and assemblage with respect to the leucocratic pockets. This leaves only a melt-related origin for the leucocratic pockets. Hollocher (2008) ruled out also this

possibility because their composition is incompatible with a melt, but this argument fails to consider that leucosome domains ~~in partially melted rocks~~ generally do not preserve a true melt composition due to interactions with the surrounding mineral phases, fractional crystallization and melt extraction ~~occurring~~ upon cooling ~~which leaves behind a more 'cumulate' material (Brown et al., 2016)~~. ~~Therefore, t~~These ~~leucocratic~~ pockets may be crystallized pods of originally trondhjemitic melt now ~~,~~ modified, a ~~during the cooling and the retrograde history of the rock; nevertheless such~~ hypothesis which however requires further investigation. Nevertheless~~If we assume that such leucocratic pods were indeed originally melt or melt-bearing pockets,~~ such pockets would ~~they can~~ only account for ≤5 melt vol%, whereas the phase equilibria modelling predicts significantly higher melt volumes (~20–25 vol.%) to be produced at the metamorphic peak conditions ~~in the garnet amphibolites~~ (Supplementary Fig. S1). The "missing" melt (15-20 vol%) could have (re)crystallized as part of the matrix, or alternatively, ~~or~~ left the source rock ~~,~~ as often observed in migmatitic terranes (e.g. Brown et al., 2016). However, evidence of significant movements of melt out of the rock are absent, and indeed both garnet amphibolites and the protolith gabbro show identical bulk compositions (except for higher H_2O in the former, McLelland and Selleck, 2011), which is overall incompatible with melt loss (see also Shinevar et al., 2021).~~.~~

4.2 Peculiar findings in nanotrondhjemites

The products visible in the Gore Mountain nanotrondhjemites often include unusual phases such as cristobalite, ~~trydimite~~tridymite and kumdykolite and, in one case, glass. The mineral phases are polymorphs of quartz and feldspar respectively, and were already

reported in nanogranitoids hosted in rocks with widely different protoliths (from ultramafic to felsic) and partially melted under extremely variable P and T conditions, i.e., low to ultrahigh P and 700 to 1100°C (Ferrero and Angel, 2018). These phases appear to be metastable products of melt crystallization resulting from "peculiar undercooled and supersaturated conditions achieved on cooling by a melt confined in a small cavity" (Ferrero and Angel, 2018 and references therein), with crystallization kinetics of the melt likely playing a fundamental role in their formation rather than P and T conditions. Polymorphs are known to disappear, i.e. revert to their most common counterparts quartz and albite in case of inclusion reopening/decrepitation (Ferrero and Angel, 2018). Thus, their persistence in inclusions can be regarded as a strong evidence that the MI are preserved and thus the melt trapped in them maintain its original composition (Bartoli and Cesare, 2020).

Glass, visible in the present study only in one partially crystallized inclusion, is commonly observed to form in volcanic rocks as result of fast cooling: however, fully and partially crystallized MI are reported in several case studies of slowly cooled regional migmatites (Cesare et al., 2015; Ferrero et al., 2018), ruling out this possibility as the only way to create glass in natural inclusions. The presence of glass can thus be regarded as another clear evidence, besides the presence of polymorphs, that metastability may be a rather common condition attained on cooling (Ferrero and Angel, 2018) in inclusions of viscous, silica-rich melt such as the ones here investigated.

4.~~2~~3 Melting at temperature in excess of 900°C in the Adirondack Highlands

~~An unexpected outcome of our study is the fact that t~~The nanotrondhjemites re-homogenize completely at T ≥~~-~~940°C and P ≥~~-~~1.0 GPa, at T higher than ~~any~~ the classic estimate of metamorphic peak T available in the Adirondack Highlands, i.e., 800-850°C and 0.65-0.86 GPa (summarized by Darling and Peck, 2016). Previous studies (Ferrero et al., 2018; 2021) have shown that the *PT* conditions at which the inclusions re-homogenize completely without evidence of decrepitation and/or melt-host interaction correspond to those of the partial melting event responsible for the formation of the inclusions (Ferrero et al., 2018 for further details). In particular, the re-homogenization T corresponds to the melting condition experienced by the rock, whereas the experimental confining P (applied to prevent MI decrepitation during re-heating) is equal to or higher with respect to the original melting P (Ferrero et al., 2018). This is also supported by a wealth of recent nanogranitoid studies where experimental *P*–*T* conditions of successful re-homogenization correspond to independently calculated partial melting conditions, e.g. classic geothermobarometry or phase equilibrium modelling (see e.g. Bartoli et al., 2013; Ferrero et al., 2018 and references therein; 2021). Thus, whereas the primary nature of the inclusions constrains the formation of garnet megacrysts at suprasolidus conditions, their re-homogenization conditions ~~suggests~~suggest ultrahigh temperature (UHT) during melting, i.e. at T in excess of 900°C. An UHT regime during garnet formation is also permissible with the results of phase equilibrium modelling (Fig. 5a, b). Phase equilibrium modelling and the similarities with previous nanogranitoid studies (Cesare et al., 2015) furthermore suggests that both melt and garnet are products of the same partial melting reaction, pointing toward a peritectic origin for the garnet megacrysts.

Although our results are at odds with the bulk of existing data on the metamorphic history of the area, we are not alone in supporting the possibility of UHT conditions in the Adirondack Highlands. Shinevar et al. (2021~~0~~) provide strong mineralogical and phase equilibria evidence in support of ultrahigh T conditions (950±40°C) ~~in samples from pit 4~~ at Barton mine, whereas recent phase equilibrium modelling on Ledge Mountain metapelitic migmatites (30 km NNW of Barton Mine) points toward metamorphic peak conditions of >~~-~~1000°C at 1.3-1.8 GPa (Davis et al., 2020). These new results call for a reappraisal of the metamorphic peak conditions experienced by the Gore Mountain garnet amphibolites and, more in general, by the rocks in the Adirondack Highlands. Further support to our interpretation that melting occurred at T > 900°C is lent by the striking similarity between what we observe in the garnet amphibolites at Barton mine and the products of mafic melting experiments. A trondhjemitic melt is indeed observed to form at T >~~-~~900°C at 1.3-1.5 GPa along with garnet, amphibole, plagioclase, clinopyroxene and orthopyroxene in melting experiments on starting compositions similar to the gabbro protolith inferred for the garnet amphibolites (Qian and Hermann, 2013; see also van der Laan and Wyllie, 1992). With the exception of clinopyroxene (probably also due to the slightly higher P ~~of used in those experimental works~~), the experimental products correspond remarkably to the phase assemblage Grt + Hbl + Pl + Opx + Melt observed in the garnet amphibolite.

4.~~3~~4 H_2O-fluxed incongruent melting in the lower crust

Incongruent melting that generates garnet in crustal rocks is generally expected to be a fluid-absent melting reaction. At Gore Mountain however the presence of a H_2O-rich

fluid is necessary to explain both melt production and the extensive hornblende growth (Fig. 1c) from metamorphism of a dry gabbro; moreover, garnet amphibolites have higher H_2O content with respect to their gabbro protolith (see paragraph 4.1). ~~. Garnet amphibolites and the protolith gabbro show identical bulk compositions, except for higher H_2O in the former (McLelland and Selleck, 2011).~~ Phase equilibrium modelling of the metagabbro at 1.0 GPa demonstrates that the growth of the observed ~13 vol.% peritectic garnet requires the influx of ~3 wt% H_2O at temperatures >~850°C (Fig. 5a, b). Thus, both modelling results and petrographic evidence point to open-system conditions during melting. Our interpretation is that the main components of gabbro (plagioclase, clinopyroxene, olivine) reacted with a H_2O-rich fluid to produce the assemblage visible in the garnet amphibolite (i.e., garnet, amphibole, plagioclase, orthopyroxene and melt), which also corresponds to the (near?) peak metamorphic assemblage visible in Fig. 5. Both presence of MI in the inner portion of garnet megacrysts and the lack of prograde zoning (Hollocher, 2008) support garnet growth entirely at (or close to) metamorphic peak conditions, i.e., at >~900°C and ~1.0 GPa.

The trace element content of the melt resembles that of the gabbro, confirming the latter as the melt source. The most notable geochemical feature of the melt is the strong enrichment in Th, U and some High Field Strength Elements (HFSE), like Zr, Hf and Ti compared to the source gabbro (Fig. 4b). At high T and lower crustal conditions, especially in presence of Na and Si (~~Wilke et al., 2012;~~ Mysen, 2015 and references therein), HFSE, U and Th can be transported in H_2O-rich fluids and subsequently transferred into the melt (Borghini et al., 2020). The melt shows a high concentration of Zr (1400 ppm average), twice the expected amount (~690 ppm) based on zircon solubility

(Boehnke et al., 2013) at the corresponding temperature and inferred major-element melt composition. Inclusions of zircon (typical host of Zr and Hf) are very rare in Gore Mountain MI, and zircon-bearing inclusions were carefully avoided during analyses. This suggests that both Zr and Hf enrichments are features of the melt itself, likely related to the increase in HFSE solubility in the presence of a free fluid (Bartels et al., 2010). Nb and Ta should be equally transported in the kind of fluid discussed here, but they are yet not as enriched as Zr-Hf-Th-U in the melt inclusions. This could be due to the growth of ilmenite (and possibly even rutile), observed as mineral inclusions in garnet, during metamorphism and melting and likely to contain a sizable amount of Nb and Ta.

In presence of an infiltrating fluid, the melt would be furthermore expected to be enriched in Large Ion Lithophile Elements (LILEs), incompatible components generally partitioned in fluids (Cannaó and Malaspina, 2018). However, in our case study LILE and HFSE appear to be decoupled, i.e., the melt shows no particular enrichment in Cs, Rb, Ba and Sr relative to the host gabbro (Fig. 4b). This may suggest a LILE-poor source, e.g. possibly related to the mantle rather than to the crust. Finally, also the H_2O-rich nature of the fluid itself is unexpected in the lower portion of an orogen undergoing collapse at the time of garnet megacrysts formation (1050 Ma; see McLelland and Selleck, 2011). The enigma represented by the fluid origin requires further studies, currently underway and involving stable isotopes investigation (Ferrero et al., in preparation).

Although the presence of a free fluid during melting of the mafic lower crust (at $P \geq 1.0$ GPa) was not regarded as a common situation (Moyen and Martin, 2012), this has been recently proposed to explain the origin of arc granitoids and the continental crust in

general (Collins et al., 2020; Pourteau et al., 2020). In the case of Gore Mountain, Goldblum and Hill (1992) suggested that the high ductility contrast between the original gabbro and the surrounding metasyenites caused the formation of a shear zone (Fig. 1b), which acted as preferential pathway for the ingress of fluid at depth.

In summary, we propose that the olivine gabbro, prior to fluid infiltration, resided in the lower part of the orogen at T in excess of 900°C without undergoing melting because of its very dry composition (0.44 wt% H_2O, McLelland and Selleck, 2011) and elevated solidus temperature, e.g. >~~–~~1000°C for this H_2O content (dashed line in Fig. 5a). The infiltration of a H_2O-rich fluid decreased significantly the solidus of the gabbro assemblage, allowing its mineral components to undergo melting, as a response to the change in H_2O content in the system. This may have taken place either at the same PT conditions present before melting or during an increase of both P and T, as recently proposed by Shinevar et al. (2021~~0~~).

4.~~4~~5 Nanotrondhjemites, experimental melts and natural TTGs

The trondhjemitic melt enclosed in the nanogranitoids of Gore Mountain is hydrous, peraluminous and with very low maficity (Table 1). The high ASI of the melt preserved at Gore Mountain cannot be ascribed to interaction with the host garnet, as evidence of chemical interaction, either chemical zoning in the garnet surrounding the re-homogenized inclusions or embayments in the inclusion walls (see ~~section~~ paragraph 4.2), are completely absent in the analyzed inclusions. The peraluminous character is consistent with the presence of osumilite as minor daughter phase in the inclusions: this phase is a rare alumina-rich, double-ring silicate found both in igneous and metamorphic

UHT rocks (Kelsey, 2008). An oddity is however the presence of amphibole as daughter mineral in the inclusions: these phases are indeed more common in metaluminous rather than peraluminous melts (Bonin et al., 2020 and references therein), and this remains an enigmatic aspect of these nanotrondhjemites.

Nanogranitoids are natural capsules where melt is trapped immediately after production and then preserved (Cesare et al., 2015), making them directly comparable to melts from mafic melting experiments in presence of H_2O (Fig. ~~7~~7~~a, b~~). The re-homogenized inclusions plot in the granitic field of the total alkali versus silica (TAS) diagram (Fig. 7a), near the most silica-rich experimental melts (e.g., Laurie and Stevens, 2012). The inclusions show a range of Na_2O values consistent with the experimental dataset on mafic melting, whereas both Ca~~e~~O (Fig. 7b) and Al_2O_3 (Fig. 7c) are generally lower than the majority of the experimental melts, in agreement with the trondhjemitic nature of the inclusions (see also the Ab-Or-An ternary diagram, Fig. 7d). In general, the ~~The~~ trapped melt~~melt~~ appears to be lower in alkalis than most experimental melts even after alkali-correction, a feature likely to contribute to the high ASI displayed by these melts (Fig. ~~7~~8~~c~~a), despite the generally low Al content of the inclusions ~~(as visible in~~ Figs. ~~7d~~8b; 7c). ~~The latter figure~~Moreover, ~~also shows how~~ the investigated nanotrondhjemites appear to represent the low-calcium, low-alumina “end-member” of the positive trend defined by the cloud of experimental melts (Fig. 8~~7db~~). The observed chemical differences could be explained by slightly different starting compositions. The Gore Mountain gabbro has a peculiar composition and is notably more mafic and showing higher Al/Ca ratio than all the starting materials from mafic melting experiments compiled here (1.13 vs. 0.63-1.01; all values are reported in Supplementary Table S4). In fact, as

part of an anorthosite suite (McLelland and Selleck, 2011), it somewhat differs in composition from expected sources for TTGs that are rather tholeiitic to transitional basalts / amphibolites (Moyen and Martin, 2012). Despite these differences, the range of ASI values found in the nanotrondhjemites is fully comparable to the experimental melts (Fig. 8~~7ca~~), indicating that the Al_2O_3, CaO, Na_2O and K_2O balance is consistent with phase relations characterizing the melting of mafic rocks.

When compared to natural TTGs, the Gore Mountain MI display higher ASI and similar AI (~~AI= (molar Al-(Na+K);~~ Fig. ~~7e~~8c) and both lower Ca and Al (Fig. ~~7f~~8d). A discrepancy is however not unexpected: as mentioned above, the source composition of the Gore Mountain MI might not be a perfect match to that of TTG magmas. In addition, these nanogranitoids contain a pristine melt trapped directly at the source region, making them necessarily different from TTG plutons/complexes, whose compositional diversity results from processes occurring in the source, during magma ascent and during emplacement. Mixing of melts from different sources and entrainment of residual or peritectic material is also recognized to increase the compositional scatter of crustal melts with respect to their starting composition measured in nanogranitoids from more felsic rocks (Bartoli et al, 2016). Moreover, magma differentiation (Smithies et al., 2019) and crystal-liquid separation during emplacement in the upper crust (Laurent et al., 2020) were recently proposed to be influential factors in shaping TTG geochemistry. In particular, the rocks composing some upper crustal TTG plutons (diorites, tonalites, trondhjemites) may represent plagioclase ± amphibole cumulates instead of true liquid compositions (Laurent et al., 2020). In fact, the Ca vs. Al compositional variability of natural TTGs is well encompassed by considering mixing in various proportions between

a liquid similar to the Gore Mountain inclusions and these two minerals (Fig. ~~7f~~8d). This model also explains the lower Si, mafic elements and higher Na concentrations of natural trondhjemites (presumably plagioclase cumulates) than the Gore Mountain nanotrondhjemites (inferred primary liquids). In this perspective, the Gore Mountain MI are “embryos” (Bartoli et al., 2014) of TTGs, in the same way that nanogranitoids in silica-rich crustal rocks are embryos of S-type granites (Bartoli et al., 2016).

4.~~5~~6 Implications for TTG petrogenesis

Although the composition of the Gore Mountain and natural TTGs may not be directly comparable in details, both bear a typical geochemical signature resulting from melting of K-poor mafic rocks, i.e., their silica-rich, trondhjemitic signature. Therefore, both can be discussed together to better constrain such melting processes, relevant to the generation of the Earth’s earliest continental crust. In studies based on natural samples, this signature is interpreted to result from melting at P ≥ 2.0 GPa in equilibrium with garnet and rutile, defining the so-called “High-Pressure” TTG (HP-TTG) group (Moyen, 2011). Thermodynamic modelling on Archean mafic rocks have recently shown that HP-TTGs may form at 900-950°C and lower P, i.e. 1.3-1.8 GPa (Kendrick and Yakymchuk, 2020) and down to 1.2 GPa (Johnson et al., 2017). Our finding shows that it is possible to form trondhjemitic melts with broadly comparable major elements signatures with HP-TTGs at similar T (≥ 925°C) and P conditions (1.0 GPa), directly from melting of lower crustal mafic rocks. Moreover, the Gore Mountain garnet amphibolite displays all the mineralogical hallmarks characteristic of residues of “low-pressure” (LP-) TTGs (i.e. formed at < 1.2 GPa, Moyen, 2011): amphibole and plagioclase are abundant, and orthopyroxene is

present instead of clinopyroxene. This apparent discrepancy between melt and residual compositions may result from a significantly different melting process than generally assumed. Although the source system is dominated by LP assemblages, the liquid itself is in equilibrium with a solid assemblage containing phases more characteristic of much deeper melting, i.e. garnet and rutile. This reflects the incongruent melting of mafic rocks, with garnet and rutile production as melting initiates, whereas this has been regarded so far in TTG petrogenesis as a mainly eutectic process, with garnet and other components of the residue being already present before the initiation of melting, and then in excess during melting (Moyen and Martin, 2012). However, the absence of relicts of sub-solidus portions in the garnet megacrysts, i.e., a clear prograde zoning, despite its pluri-decimetric size supports the evidence that these porphyroblasts started growing only at the onset of the melting, similarly to what was observed in experiments on mafic rocks (Beard and Lofgren, 1991) and other systems (Patiño Douce and Harris, 1998).

Conversely, the trace element concentrations of Gore Mountain MI show contrasting LP-like and HP-like features. Sr and LREE contents are fully compatible with LP-TTGs (Fig. 94a), whereas Nb and Ta are very low, as typically ascribed to HP-TTGs (Fig. 94b, c) due to the presence of rutile and ilmenite as well as amphibole (for Nb) in the residue. Thermodynamic calculations on Archean basalts (Johnson et al., 2017) have shown that TTGs with garnet + rutile residue may indeed form at P as low as 1.2 GPa, typical of LP-TTGs, thus supporting the idea that LP melts from mafic melting can share features with HP-TTGs. This requires a careful re-evaluation of the existent databases, insofar as some TTGs currently classified as HP-TTGs based on Nb and Ta contents should be instead classified as LP-TTGs.

5. Conclusions

The garnet megacrysts of Barton mine at Gore Mountain have been attracting the attention of expert scientific audience and general public alike since their discovery in the 1850's (Kelly and Darling, 2008) because of their unparalleled size. This feature swayed the attention of most of the scientific community toward the macroscale features of these crystals, at the expenses of ~~high resolution~~high-resolution studies in the garnet interiors (with the remarkable exception of Shinevar et al. 2021). Our work shows how novel insights into geological processes with both local and worldwide relevance can be gained from the study of the microstructural features of such ~~remarkable~~ rocks. Our petrographic, experimental and modelling results prove for the first time ~~how~~ that these garnets are peritectic and preserve micrometric droplets of trondhjemitic melt. Such melt results from the H_2O-fluxed melting of a gabbro in the lower crust during ultrahigh temperature metamorphism, a condition only recently recognized in the Adirondack Highlands (Shinevar et al., 2021) and still controversial ~~(W. Shinevar, pers.comm.)~~. Further studies are needed to relate our solid microstructural and microchemical constraints to the geodynamic evolution of the area during the late Mesoproterozoic.

The compositional similarity between the trondhjemitic MI and TTGs provides us with the possibility to directly investigate the composition of the trondhjemitic melt, the phases coexistent with it as well as its mafic source rock, generated under well-constrained conditions. Our work shows how H_2O-fluxed partial melting of mafic crust creates TTG-like melts with "HP-like" major elements and hybrid traces, i.e., "LP-like" in Sr and Ce contents and~~,~~ "HP-like" in Nb and Ta. Previously thought to be smoking guns

of different melting P (at crustal versus mantle depths), such contrasting features within a single melt inclusion demonstrates that trace element signatures of TTGs are not diagnostic of depth of melting and geodynamic setting (see also Smithies et al., 2019). This result is complementary to recent findings that crystal-liquid segregation in TTG plutons can result in similar discrepancies (Laurent et al., 2020), pointing out that both source processes (melting reaction, H_2O activity) and magma chamber dynamics exert a first-order control on TTG geochemistry, instead of melting pressure. Our finding provides support to ~~also strengthens~~ the idea of a two-stage mechanism of TTG production (Moyen and Martin, 2012), i.e., mantle melting to produce basalt/gabbro, followed by melting of basalt/gabbro at lower crustal conditions to produce the TTG parental magma. This does not invalidate however other TTG production models, i.e. ~~–~~a one-stage mechanism whereby TTGs are produced by direct fractional crystallization of hydrous basalts (Jagoutz et al., 2013), which remain a valid explanation for occurrences where TTG granitoids are associated with magmatic cumulates in the lower crust~~, rather than a one-stage mechanism whereby TTGs are produced by direct fractional crystallization of hydrous basalts (Jagoutz et al., 2013)~~.

In conclusion, these TTG embryos are ~~the first~~a direct natural evidence that melting of mafic rocks generates TTG-like melts, in agreement with previous research (e.g., Jonhson et al., 2012; Porteau et al., 2020), and that such melts can be found in the source region as MI. It is arguable that the production of TTG-like melts at Gore Mountain is the result of a peculiar set of circumstance of local significance, i.e., local H_2O-rich fluid infiltration at depth. Nevertheless, H_2O-fluxed melting of lower crustal mafic rocks is increasingly recognized as a fundamental process for the production of TTGs, thus

lending to our findings a clear and undoubtable relevance for the advancement of our understanding of TTG petrogenesis.

Acknowledgements

Our deepest thanks go to Bonnie Barton for being an outstanding guide during our visit to Barton Mines. The present research was funded by the German Federal Ministry for Education and Research and the Deutsche Forschungsgemeinschaft (Project FE 1527/2-2) to SF. We are grateful to C. Günter, M.A. Ziemann, F. Wilke, F. Kaufmann and L. Hecht for help during analyses and to C. Fischer for sample preparation. ~~Our deepest thanks go to Bonnie Barton for being an outstanding guide during our visit to Barton Mines.~~ The comments of T. Tacchetto and other anonymous reviewers on an earlier (shorter) version, and of O. Jagoutz and T. Johnson on the latest version ~~thoughtful inputs of T. Tacchetto and other reviewers on a previous shorter version of the present paper~~ lead to an improvement ~~significant increase~~ in both ~~of the~~ clarity and significance of the present manuscript.

References

Bartels, A., Holtz, F., and Linnen, R. L., 2010, Solubility of manganotantalite and manganocolumbite in pegmatitic melts: American Mineralogist, v. 95 (4), p. 537-544, https://doi.org/10.2138/am.2010.3157.

Bartoli, O., Cesare, B., Poli, S., Acosta-Vigil, A., Esposito, R., Turina, A., Bodnar, R. J., Angel, R. J., and Hunter, J., 2013, Nanogranite inclusions in migmatitic garnet:

behavior during piston-cylinder remelting experiments: Geofluids, 13, p. 405-420, https://doi.org/10.1111/gfl.12038.

Bartoli, O., Cesare, B., Remusat, L., Acosta-Vigil, A., and Poli, S, 2014, The H_2O content of granite embryos: Earth and Planetary Science Letters, v. 395, p. 281–290, https://doi.org/10.1016/j.epsl.2014.03.031.

Bartoli, O., Acosta-Vigil, A., Ferrero, S., and Cesare, B., 2016, Granitoid magmas preserved as melt inclusions in high-grade metamorphic rocks: American Mineralogist, v. 101, p. 1543–1559, https://doi.org/10.2138/am-2016-5541CCBYNCND.

Bartoli, O., and Cesare, B., 2020. Nanorocks: a 10 year old story: Rendiconti Lincei. Scienze Fisiche e Naturali, v. 31, p. 249-257, https://doi.org/10.1007/s12210-020-00898-7.

Baxter, E. F., Caddick, M. J., and Ague, J. J., 2013, Garnet: Common mineral, uncommonly useful. Elements, v. 9(6), p. 415-419.

Beard, J. S., and Lofgren, G. E., 1991, Dehydration melting and water-saturated melting of basaltic and andesitic greenstones and amphibolites at 1, 3, and 6. 9 kb: Journal of Petrology, v. 32, p. 365-401, https://doi.org/10.1093/petrology/32.2.365.

Boehnke, P., Watson, B. E., Trail, D., Harrison, T. M., and Schmitt, A. K., 2013, Zircon saturation re-revisited: Chemical Geology, v. 351, p. 324–334, https://doi.org/10.1016/j.chemgeo.2013.05.028.

Bonin, B., Janoušek, V., and Moyen, J.-F:, 2020, Chemical variation, modal composition and classification pf granitoids, *in* Janoušek, V., Bonin, B., Collins, W.J., Farina, F., and Bowden, P., eds., Post-Archean Granitic Rocks: Petrogenetic Processes and Tectonic Environments: Geological Society, London, Special Publications, v. 491, p. 9-51, https://doi.org/10.1144/SP491-2019-138.

Borghini, A., Ferrero, S., O'Brien, P. J., Laurent, O., Günter, C., and Ziemann, M. A., 2020, Cryptic metasomatic agent measured in situ in Variscan mantle rocks: Melt inclusions in garnet of eclogite, Granulitgebirge, Germany: Journal of Metamorphic Geology, v. 38, p. 207–234, https://doi.org/10.1111/jmg.12519.

Brown, C. R., Yakymchuk, C., Brown, M., Fanning, C. M., Korhonen, F. J., Piccoli, P. M., and Siddoway, –2016, From Source to Sink: Petrogenesis of Cretaceous Anatectic Granites from the Fosdick Migmatite – Granite Complex, West ~~Antartica~~Antarctica: Journal of Petrology, v. 57 (7), p. 1241-1278, https://doi.org/10.1093/petrology/egw039.

Cannaó, E., and Malaspina, N., 2018, From oceanic to continental subduction: Implications for the geochemical and redox evolution of the supra-subduction mantle: Geosphere, v. 14, no. 6, p. 2311-2336, https:// doi .org /10 .1130 /GES01597 .1.

Cesare, B., Acosta-Vigil, A., Bartoli, O., and Ferrero, S., 2015, What can we learn from melt inclusions in migmatites and granulites? Lithos, v. 239, p. 186-216, https://doi.org/10.1016/j.lithos.2015.09.028.

Collins, W. J., Murphy, J. B., Johnson, T. E., and Huang, H.-Q., 2020, Critical role of water in the formation of continental crust: Nature Geoscience, v. 13, p. 331-338, https://doi.org/10.1038/s41561-020-0573-6.

Darling, R. S., 2013, Zircon-bearing, crystallized melt inclusions in peritectic garnet from the western Adirondack Mountains, New York State, USA: Geofluids, v. 13 (4), p. 453-459, https://doi.org/10.1111/gfl.12047.

Darling, R. S., Chou, I.-M., and Bodnar, R. J., 1997, An occurrence of metastable cristobalite in high-pressure garnet granulite: Science, v. 276, p. 91–93, https://doi.org/10.1126/science.276.5309.91.

Darling, R.S. and Peck, W.H., 2016, Metamorphic conditions of Adirondack rocks: Adirondack Journal of Environmental Studies, v. 21, Article 7.

Davis, M., Leech, M. and Metzger, E.P., 2020, Determining the Petrotectonic Evolution of Ledge Mountain Migmatites with Phase Equilibria Modelling and Melt Reintegration: Adirondack Highlands, New York. Abstract V019-0004 presented at 2020 Fall Meeting, AGU, San Francisco, CA, 1-17 Dec.

Ferrero, S., and Angel, R. J., 2018, Micropetrology: are inclusions in minerals grains of truth? Journal of Petrology, v. 59, p. 1671–1700, doi: 10.1093/petrology/egy075.~~Ferrero, S., Ziemann, M. A., Angel, R. J., O'Brien, P. J., and Wunder, B., 2016, Kumdykolite, kokchetavite, and cristobalite crystallized in nanogranites from felsic granulites, Orlica–Snieznik Dome (Bohemian Massif): not evidence for ultrahigh-pressure conditions: Contributions to Mineralogy and Petrology, v.171, p. 1-12, https://doi.org/10.1007/s00410-015-1220-x.~~

678 Ferrero, S., O'Brien, P. J., Borghini, A., Wunder, B., Wälle, M., Günter, C., and
679 Ziemann, M. A., 2018, A treasure chest full of nanogranitoids: an archive to
680 investigate crustal melting in the Bohemian Massif, *in* Ferrero, S., Lanari, P.,
681 Goncalves, P., and Grosch, E. G., eds., Metamorphic Geology: Microscale to
682 Mountain Belts: Geological Society, London, Special Publications 478, p. 13-38,
683 https://doi.org/10.1144/SP478.19.

684 Ferrero, S., Ague, J.J., O'Brien, P.J., Wunder, B., Remusat, L., Ziemann, M.A., Axler,
685 J., 2021, High pressure, halogen-bearing melt preserved in ultra-high temperature
686 felsic granulites of the Central Maine Terrane, Connecticut (US): American
687 Mineralogist, in press, https://doi.org/10.2138/am-2021-7690.

688 Forshaw, J. B., Waters, D. J., Pattison, D. R. M., Pallin, R., and Gopon, P., 2019, A
689 comparison of observed and thermodynamically predicted phase equilibria and
690 mineral compositions in mafic granulites: Journal of Metamorphic Geology, v. 37,
691 p. 153-179, https://doi.org/10.1111/jmg.12454.

692 Goldblum, D. R., and Hill, M. L., 1992, Enhanced fluid flow resulting from competency
693 contrast within a shear zone: The garnet ore zone at Gore Mountain, N.Y: The
694 Journal of Geology, v. 100, p. 776–782, https://doi.org/10.1086/629628.

695 Hollocher, K., 2008, Origin of big garnets in amphibolites during high-grade
696 metamorphism, Adirondacks, New York: 21st Annual Keck Undergraduate
697 Research Symposium,- p. 129–134.

698 Jagoutz, O., Schmidt, M. W., Enggist, A., Burg, J.-P., Hamid, D., and Hussain, S.,
699 2013, TTG-type plutonic rocks formed in a modern arc batholith by hydrous

fractionation in the lower arc crust: Contributions to Mineralogy and Petrology, v. 166(4), p. 1099-1118, https://doi.org/10.1007/s00410-013-0911-4.

Johnson, T. E., Brown, M., Kaus, B. J. P., and VanTongeren, J. A., 2013, Delamination and recycling of Archaean crust caused by gravitational instabilities: Nature Geoscience, v. 7, p. 47–52, https://doi.org/10.1038/ngeo2019.

Johnson, T. E., Brown, M., Gardiner, N. J., Kirkland, C. L., and Smithies, R. H., 2017, Earth's first stable continents did not form by subduction: Nature, v. 543, p. 239–242, https://doi.org/10.1038/nature21383.

Johnson, T. E., Fischer, S., White, Brown, M., Rollinson, H.R., 2012, Archaean intracrustal differentiation from partial melting of metagabbro—field and geochemical evidence from the central region of the Lewisian complex, NW Scotland: Journal of Petrology, v. 53 (10), p. 2115–2138. https://doi.org/10.1093/petrology/egs046

Johnston, A. D., and Wyllie, P. J., 1988, Constraints on the origin of Archean trondhjemites based on phase relationships of Nûk gneiss with H_2O at 15 kbar: Contributions to Mineralogy and Petrology, v. 100, p. 35-46, https://doi.org/10.1007/BF00399438.

Kelly, W.M., and Darling, R. S., 2008, Geology and mining history of the Barton garnet mine, Gore Mt., and the NL ilmenite mine, Tahawus, NY with a temporal excursion to the Macintyre, *in* Selleck, B.W., 80th Annual Meeting of the New York State Geological Association, Fieldtrip Guidebook, 154 p.

721 Kelsey, D. E., 2008, On ultrahigh-temperature crustal metamorphism: Gondwana
722 Research, v. 13 (1), p. 1-29, https://doi.org/10.1016/j.gr.2007.06.001.

723 Kendrick, J., and Yakymchuk, C., 2020, Garnet fractionation, progressive melt loss
724 and bulk composition variations in anatectic metabasites: Complications for
725 interpreting the geodynamic significance of TTGs: Geoscience Frontiers, v. 11, p.
726 745-763, https://doi.org/10.1016/j.gsf.2019.12.001.

727 Lanari, P. and Duesterhoeft, E., 2019, Modelling metamorphic rocks using equilibrium
728 thermodynamics and internally consistent databases: past achievements, problems
729 and perspectives: Journal of Petrology, 60(1), p.19-56,
730 https://doi.org/10.1093/petrology/egy105.

731 Laurent, O., Björnsen, J., Wotzlaw, J.-F., Bretscher, S., Pimenta Silva, M., Moyen, J.-
732 F., Ulmer, P., and Bachmann, O., 2020, Earth's earliest granitoids are crystal-rich
733 magma reservoirs tapped by silicic eruptions: Nature Geoscience, v. 13(2), p. 163-
734 169, https://doi.org/10.1038/s41561-019-0520-6.

735 Laurie, A., and Stevens, G., 2012, Water-present eclogite melting to produce Earth's
736 early felsic crust: Chemical Geology, v. 314–317, p. 83–95,
737 https://doi.org/10.1016/j.chemgeo.2012.05.001.

738 McLelland, J. M., and Selleck, B. W., 2011, Megacrystic Gore Mountain–type garnets
739 in the Adirondack Highlands: Age, origin, and tectonic implications: Geosphere, v.
740 7, p. 1194–1208, https://doi.org/10.1130/GES00683.1.

741 Moyen, J.-F., 2011, The composite Archaean grey gneisses: Petrological significance,
742 and evidence for a non-unique tectonic setting for Archaean crustal growth: Lithos,
743 v. 123(1-4), p. 21-36, https://doi.org/10.1016/j.lithos.2010.09.015.

744 Moyen, J.-F., and Martin, H., 2012, Forty years of TTG research: Lithos, v. 148, p.
745 312–336, https://doi.org/10.1016/j.lithos.2012.06.010.

746 Mysen, B., 2015, An in situ experimental study of Zr^{4+} transport capacity of water-rich
747 fluids in the temperature and pressure range of the deep crust and upper mantle:
748 Progress in Earth and Planetary Science, v. 2, 38, https://doi.org/10.1186/s40645-
749 015-0070-5.

750 Nicoli, G., and Ferrero, S., 2021, Nanorocks, volatiles and plate tectonics: Geoscience
751 Frontiers, ~~under review~~accepted.

752 Patiño Douce, A. E., and Harris, N., 1998, Experimental constraints on Himalayan
753 anataxis: Journal of Petrology, v. 39(4), p. 689-710,
754 https://doi.org/10.1093/petroj/39.4.689.

755 Pourteau, A., Ducet, L. S., Blereau, E. R., Volante, S., Johnson, T. E., Collins, W. J.,
756 Li, Z.-X., and Champion, D. C., 2020, TTG generation by fluid-fluxed crustal
757 melting: Direct evidence from the Proterozoic Georgetown Inlier, NE Australia, v.
758 550, https://doi.org/10.1016/j.epsl.2020.116548.

759 Qian, Q., and Hermann, J., 2013, Partial melting of lower crust at 10–15 kbar:
760 constraints on adakite and TTG formation: Contributions of Mineralogy and
761 Petrology, v. 165, p. 1195–1224, https://doi.org/10.1007/s00410-013-0854-9.

762 Rivers, T., 1997, Lithotectonic elements of the Grenville Province: review and tectonic
763 implications: Precambrian Research, v. 167, p. 117-154,
764 https://doi.org/10.1016/S0301-9268(97)00038-7.

765 Shinevar, W.J., Jagoutz, O., and VanTongeren, J.A., ~~2020~~2021, Gore Mountain
766 Garnet Amphibolite records UHT Conditions: Implications for the Rheology of the
767 Lower Continental Crust During Orogenesis~~Gore Mountain Garnet Amphibolite~~
768 ~~Records UHT Conditions: Implications for the Rheology of the Lower Continental~~
769 ~~Crust During Orogenesis,~~: Journal of Petrology, accepted,
770 https://doi.org/10.1093/petrology/egab007~~in Geological Society of America~~
771 ~~Abstracts, 2020~~.

772 Smithies, R. H., Lu, Y., Johnson, T., Kirkland, C. L., Cassidy, K. F., Champion, D. C.,
773 Mole, D. R., Zibra, I., Gessner, K., Sapkota, J., De Paoli, M. C., and Poujol, M.,
774 2019, No evidence for high-pressure melting of Earth's crust in the Archean:
775 Nature Communications, v. 10, 5559, https://doi.org/10.1038/s41467-019-13547-
776 x.

777 van der Laan, S. R., and Wyllie, P. J., 1992, Constraints on Archean Trondhjemite
778 Genesis from Hydrous Crystallization Experiments on Nûk Gneiss at 10-17 kbar:
779 The Journal of Geology, v. 100, p. 57-68.

780 ~~Wilke, M., Schmidt, C., Dubrail, J., Appel, K., Borchert, M., Kvashnina, K., and~~
781 ~~Manning, C. M., 2012, Zircon solubility and zircon complexation in~~
782 ~~$H_2O+Na_2O+SiO_2±Al_2O_3$ fluids at high pressure and temperature: Earth Planetary~~
783 ~~Science Letters, v. 349–350, p. 15–25, https://doi.org/10.1016/j.epsl.2012.06.054.~~

784 White, R.W., Stevens, G. and Johnson, T.E., 2011. Is the crucible reproducible?
785 Reconciling melting experiments with thermodynamic calculations. Elements, 7(4),
786 p. 241-246.

787 Winther, T. K., 1996, An experimentally based model for the origin of tonalitic and
788 trondhjemitic melts: Chemical Geology, v. 127, p. 43–59,
789 https://doi.org/10.1016/0009-2541(95)00087-9.

790 Winther, T. K., and Newton, R. C., 1991, Experimental melting of a hydrous low-K
791 tholeiite: evidence on the origin of Archaean cratons: Bulletin of the Geological
792 Society of Denmark, v. 39.

793

Captions

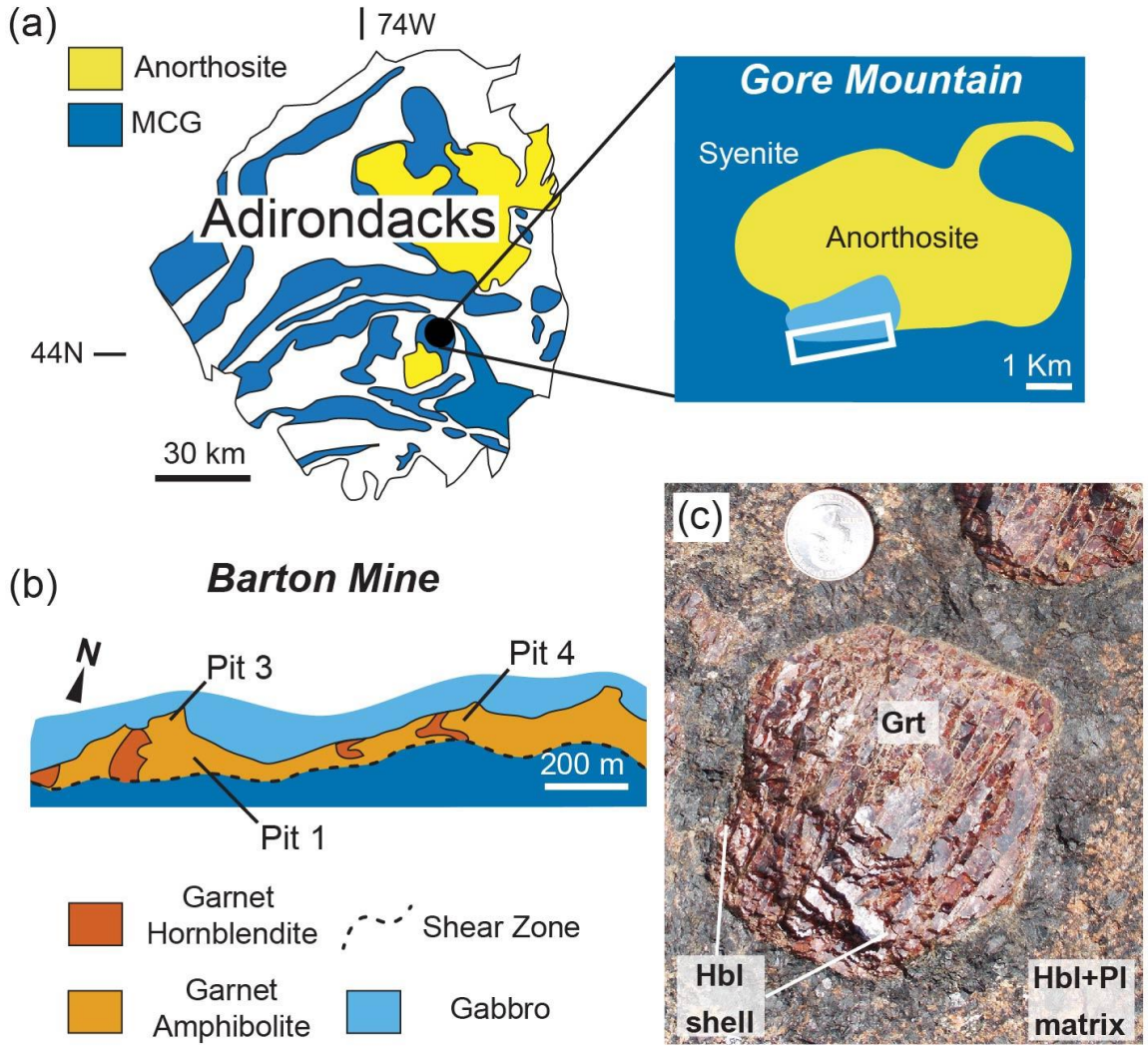

Fig. 1. a) Simplified geological setting (modified after McLelland and Selleck, 2011) of the Adirondacks (NY state, US) showing the rock types of interest. MCG= mangerite-charnockite-granite suite. ~~Red~~ Black dot= location of Gore Mountain, with general geologic setting in the inset on the right. White box= location of Barton Mine. (b) Detailed geological map of the open pit of Barton Mine. The inclusion-bearing garnets investigated in this study are from the garnet amphibolites; the garnet hornblendites present along with the amphibolites have smaller garnets hosted in a matrix of pluri-cm hornblende, and

were not investigated in the present study. The location of the shear zone is based on Goldblum and Hill (1992). (c) Garnet (Grt) megacryst surrounded by hornblende (Hbl) in a matrix of Hbl and plagioclase (Pl) and minor orthopyroxene, not visible in the figure. Coin diameter= 2.5 cm.

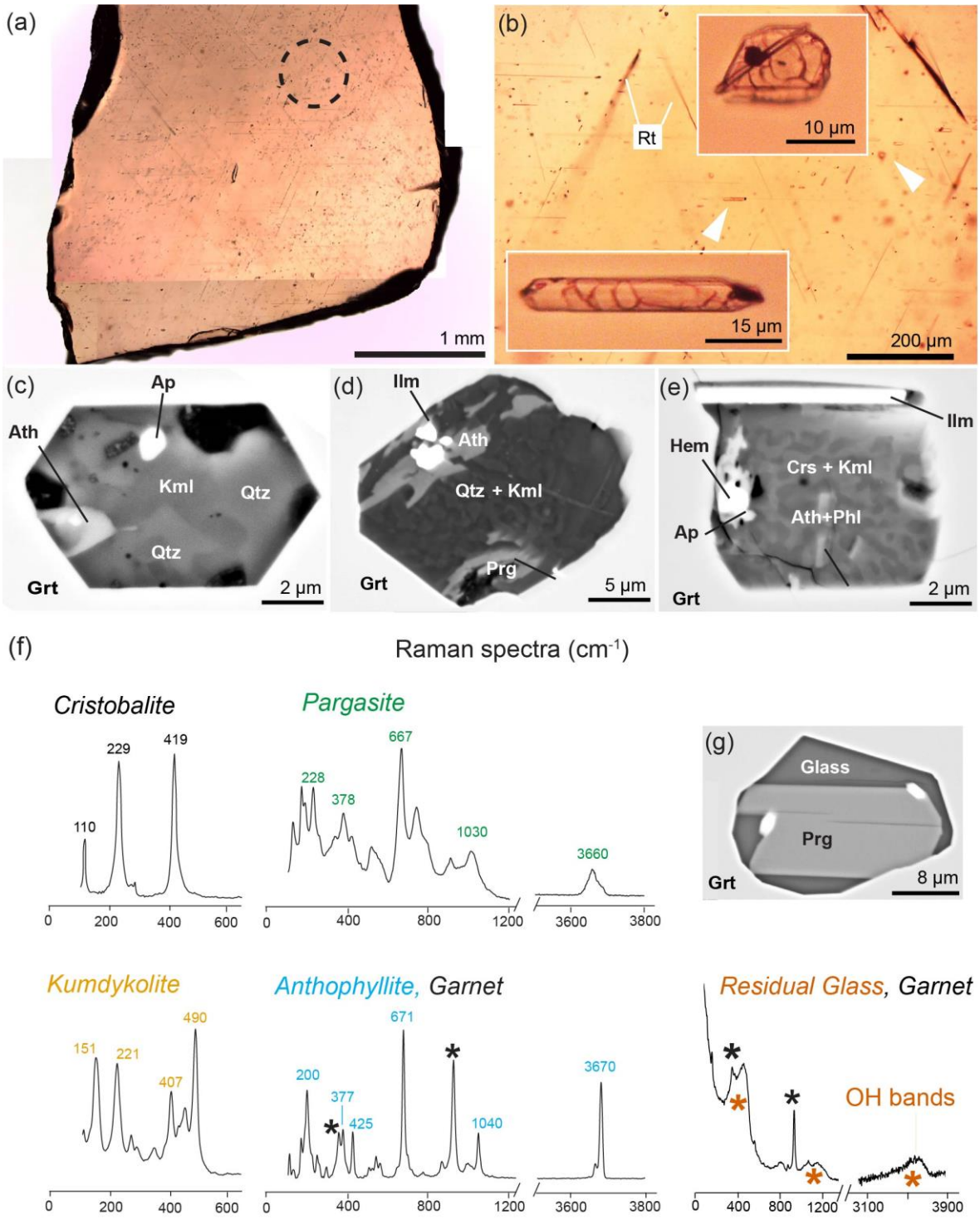

807

808 Fig. 2. Crystallized and partially crystallized melt inclusions in Gore Mountain megacrysts.

809 (a) Inclusion-bearing, doubly-polished chips of garnet megacrysts. Dashed circle=

810 location of fig. (b). (b) close up of the garnet chip with enlargements of isometric and

tubular inclusions. Rt= rutile needles. (c), (d) and (e) back scattered electron (BSE) images of the inclusions. Ath=anthophyllite, Kml=kumdykolite, Crs= Cristobalite; Qtz= quartz, Ap=apatite, Ilm=ilmenite, Prg=pargasite, Phl=phlogopite and Hem=hematite. In (d) and (e) kumdykolite and quartz/cristobalite show a typically igneous micrographic texture. (f) MicroRaman spectra of the crystalline phases in inclusions as well as glass. (g) Partially crystallized inclusion with MicroRaman spectrum of the glass visible in (f).

(a)

		Experimental runs				
Parameters						
T(°C)	900	925	940	940	940	950
P (GPa)	1.0	1.0	1.0	1.5	1.5	1.0
t (h)	24	24	24	24	24	24
Results						
Re-melting	-	Limited	+	+	+	+
Re-hom.	-	MI <2µm	+	+	+	+
Cracks	-	Rare	Rare	+	Rare	+
Interaction	-	-	-	-	-	+
Name	GM3	GM5	GM7	GM8	GM9	GM1

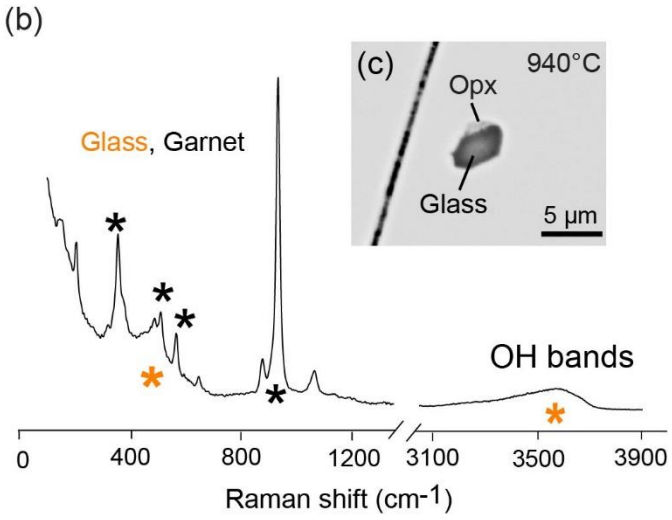

Fig. 3. Experimental re-homogenization of the inclusions. (a) Table reporting the parameters used in the re-homogenization experiments at the piston cylinder press, with relevant microstructural observations. In gray we report the two experiments where the inclusions were analyzed to obtain the composition of the original melt (Table 1). (b) Raman spectrum of the glass inside a fully re-homogenized nanogranitoid, visible in figure (c), next to an orthopyroxene interpreted as already coexisting with the melt during garnet growth and inclusion formation (see text for details).

Experiment	GM7	GM7	GM9	GM9	GM9	GM9	GM9			
No.	28	25	32-32	33	24	31	22-23	*Average*	St.Dev	Residual Glass
Trapped phases	None	Opx	Opx	Opx	Opx	Opx+Crs+Ilm	Opx			
SiO_2	69.70	71.79	75.81	73.79	72.04	72.30	67.79	*71.89*	2.06	77.58
TiO_2	0.06	0.64	0.34	0.22	0.34	0.38	0.33	*0.33*	0.19	0.01
Al_2O_3	12.93	11.36	11.46	13.43	12.52	13.57	12.82	*12.58*	0.95	12.92
FeO	3.54	4.47	2.43	4.84	3.51	2.59	2.91	*3.47*	0.97	0.80
MnO	0.04	0.00	0.07	0.12	0.07	0.01	0.01	*0.05*	0.04	0.00
MgO	1.72	2.54	0.50	1.62	1.70	1.00	0.72	*1.40*	0.70	0.06
CaO	1.80	1.38	0.92	1.78	1.72	1.52	1.55	*1.52*	0.34	0.07
Na_2O	3.02	2.21	3.49	4.22	3.86	5.55	3.86	*3.74*	1.14	4.53
K_2O	1.34	0.44	0.31	0.25	0.38	0.20	1.81	*0.67*	0.43	3.25
P_2O_5	0.02	0.20	0.07	0.00	0.00	0.10	0.03	*0.06*	0.08	0.02
Cl	0.00	0.00	0.03	0.02	0.00	0.00	0.26	*0.05*	0.01	0.00
Total	94.18	95.02	95.43	100.29	96.12	97.22	92.09	*95.77*	2.17	99.25
Q	38	48	50	38	39	33	32	*40*	7	38
C	3	5	4	3	3	2	2	*3*	1	2
Or	8	3	2	1	2	1	11	*4*	4	19
Ab	26	19	29	36	33	47	33	*32*	9	38
An	9	6	4	9	9	7	7	*7*	2	0
Hy	11	13	5	13	10	7	7	*9*	3	2
Mg#	0.46	0.50	0.26	0.37	0.46	0.41	0.30	*0.39*	0.09	0.11
ASI	1.33	1.72	1.48	1.29	1.27	1.12	1.15	*1.34*	0.21	1.16
AI	0.064	0.071	0.053	0.061	0.057	0.041	0.044	*0.06*	0.01	0.02
Na_2O/CaO	0.44	0.20	0.09	0.06	0.10	0.04	0.47	*0.20*	0.17	0.72
Al/Na+K	2.01	2.77	1.89	1.86	1.85	1.45	1.54	*1.91*	0.43	1.18
K_2O/Na_2O	1.68	1.60	3.78	2.37	2.25	3.65	2.48	*2.54*	0.87	68.0
maficity	0.09	0.13	0.05	0.11	0.09	0.06	0.06	*0.08*	0.03	0.01
H_2O by diff	5.82	4.99	4.60	-0.27	3.88	2.79	8.17	*4.28*	2.62	0.75
K#	0.23	0.12	0.06	0.04	0.06	0.02	0.24	*0.11*	0.09	0.32

826

(n=7)	Average	*St.Dev*	Residual Glass
SiO_2	71.89	*2.61*	77.58
TiO_2	0.33	*0.17*	0.01
Al_2O_3	12.58	*0.88*	12.92
FeO	3.47	*0.92*	0.80
MnO	0.05	*0.04*	0.00
MgO	1.40	*0.70*	0.06
CaO	1.52	*0.31*	0.07
Na_2O	3.74	*1.04*	4.53
K_2O	0.67	*0.63*	3.25
P_2O_5	0.06	*0.07*	0.02
Cl	0.05	*0.10*	0.00
Total	95.77	*2.56*	7.80
Q	40	*7*	38
C	3	*1*	2
Or	4	*4*	19
Ab	32	*9*	38
An	7	*2*	0
Hy	9	*3*	2
Mg#	0.39	*0.09*	0.11
ASI	1.34	*0.21*	1.16
AI	0.06	*0.01*	0.02
K/N	0.20	*0.17*	0.72
A/NK	1.91	*0.43*	1.18
N/C	2.54	*0.87*	68.0
maficity	0.08	*0.03*	0.01
H_2O by diff	4.28	*2.62*	0.75
K#	0.11	*0.09*	0.32

Table 1. Microchemical analyses of MI and residual glass~~Glass compositions~~. The MI compositions were measured after experimental re-homogenization via EMP analyses. See “methods” for the alkali correction procedure. AI= Alkalinity Index (AI=molar Al-(Na+K)); ~~M~~maficity = total FeO and MgO contents expressed as atomic Fe + Mg; potassium number (K#) = [molar K_2O/ (K_2O + Na_2O)]. Crs= cristobalite; Opx= Orthopyroxene. ~~The complete dataset is visible in Table S2.~~

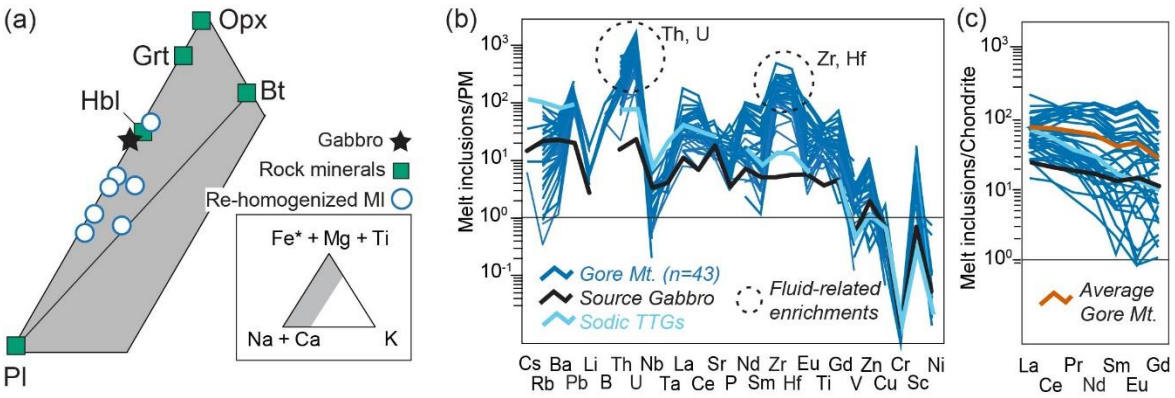

Fig. 4: Chemistry of the melt in inclusions. (a) Re-homogenized inclusion composition versus gabbro protolith (from McLelland and Selleck, 2011) and mineral phase composition in the garnet amphibolite. (b) Primitive mantle (PM)-normalized pattern of MI trace elements (Table S23) versus source rock and sodic TTGs average. (c) Chrondrite-normalized REE patterns of MI. Y and Heavy REE (HREE) contents of the MI are not available due to limitations of the deconvolution (see Methods and text). The dataset does not include MI with trapped phases such as rutile, ilmenite, zircon and apatite. Sodic TTGs composition is from Moyen and Martin (2012). For details on "fluid-related enrichments" see section 4.4.

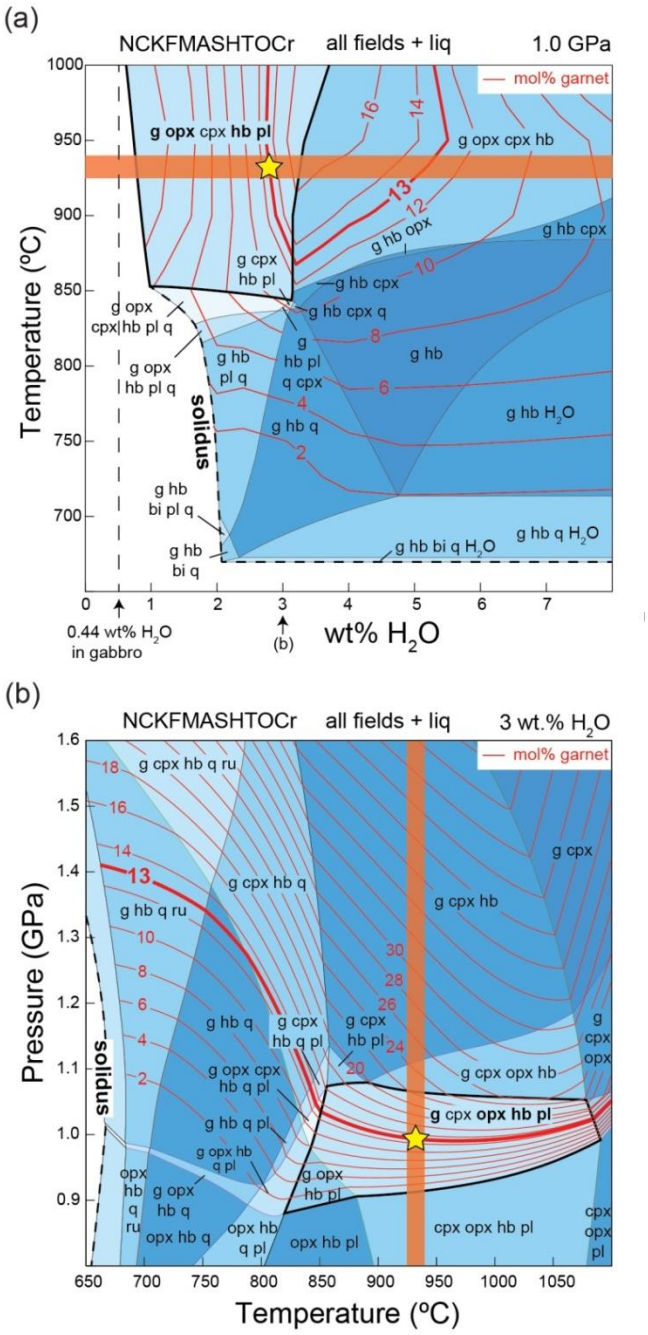

Fig. 5: Results of phase equilibrium modelling: (a) T - wt% H_2O diagram at 1.0 GPa, and (b) *P-T* diagram with 3wt% H_2O, also indicated in (a). Orange box = T range at which the inclusions can be successfully re-homogenized, 925-940°C. Yellow star = *PT* conditions of garnet megacrysts formation as result of melting, also corresponding to melt entrapment.

852 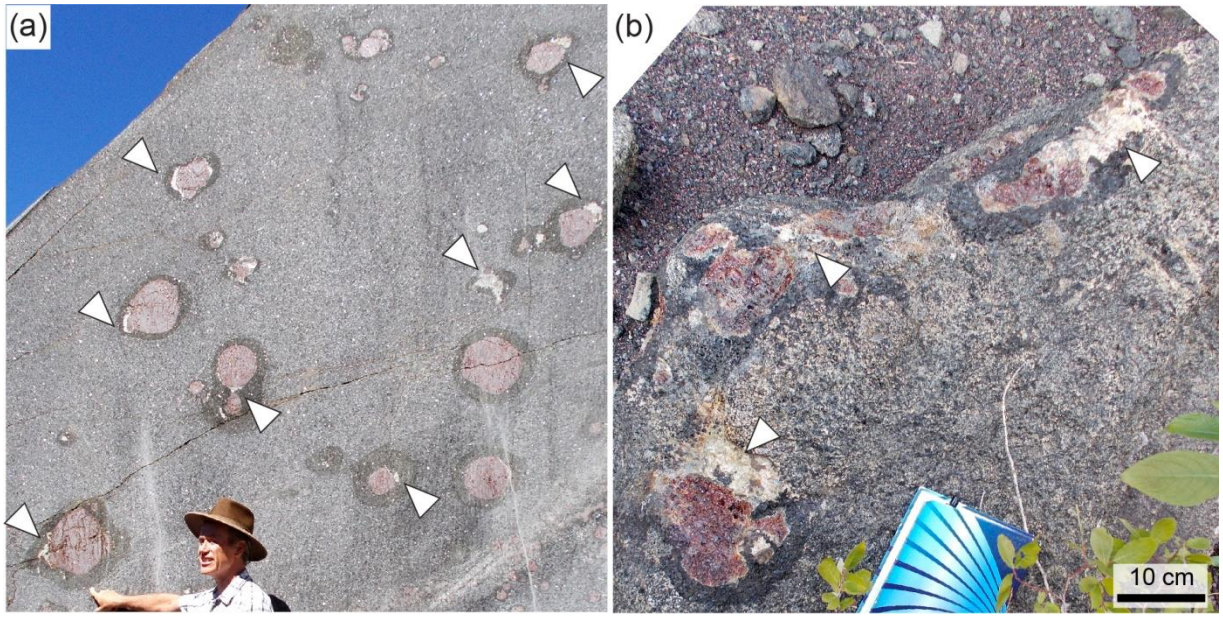

853 Fig. 6: Possible outcrop evidence for the former presence of melt. White arrows =
854 leucocratic pockets. (a) Freshly cut surface (August 2018) located in pit 3 (. (b) Loose
855 boulder in the lower part of pit 1.

856

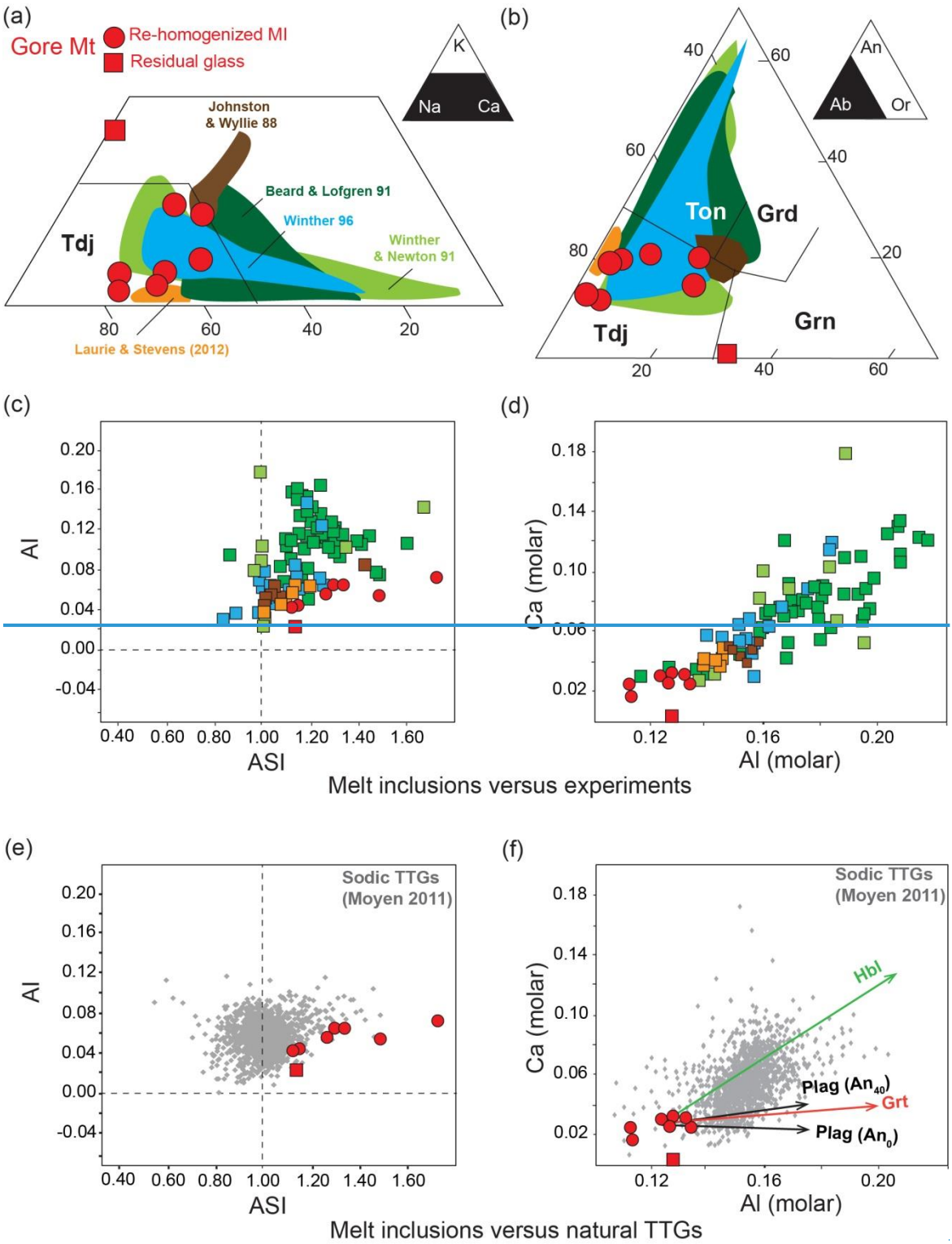
(a)
Gore Mt
Re-homogenized MI
Residual glass
K
Na
Ca
Johnston & Wyllie 88
Beard & Lofgren 91
Winther 96
Winther & Newton 91
Tdj
80
60
40
20
Laurie & Stevens (2012)
(b)
An
Ab
Or
40
60
60
40
80
20
Ton
Grd
Tdj
Grn
20
40
60
(c)
AI
0.20
0.16
0.12
0.08
0.04
0.00
-0.04
0.40 0.60 0.80 1.00 1.20 1.40 1.60
ASI
(d)
Ca (molar)
0.18
0.14
0.10
0.06
0.02
0.12 0.16 0.20
Al (molar)
Melt inclusions versus experiments
(e)
Sodic TTGs (Moyen 2011)
AI
0.20
0.16
0.12
0.08
0.04
0.00
-0.04
0.40 0.60 0.80 1.00 1.20 1.40 1.60
ASI
(f)
Sodic TTGs (Moyen 2011)
Ca (molar)
0.18
0.14
0.10
0.06
0.02
Hbl
Plag (An40)
Grt
Plag (An0)
0.12 0.16 0.20
Al (molar)
Melt inclusions versus natural TTGs

857

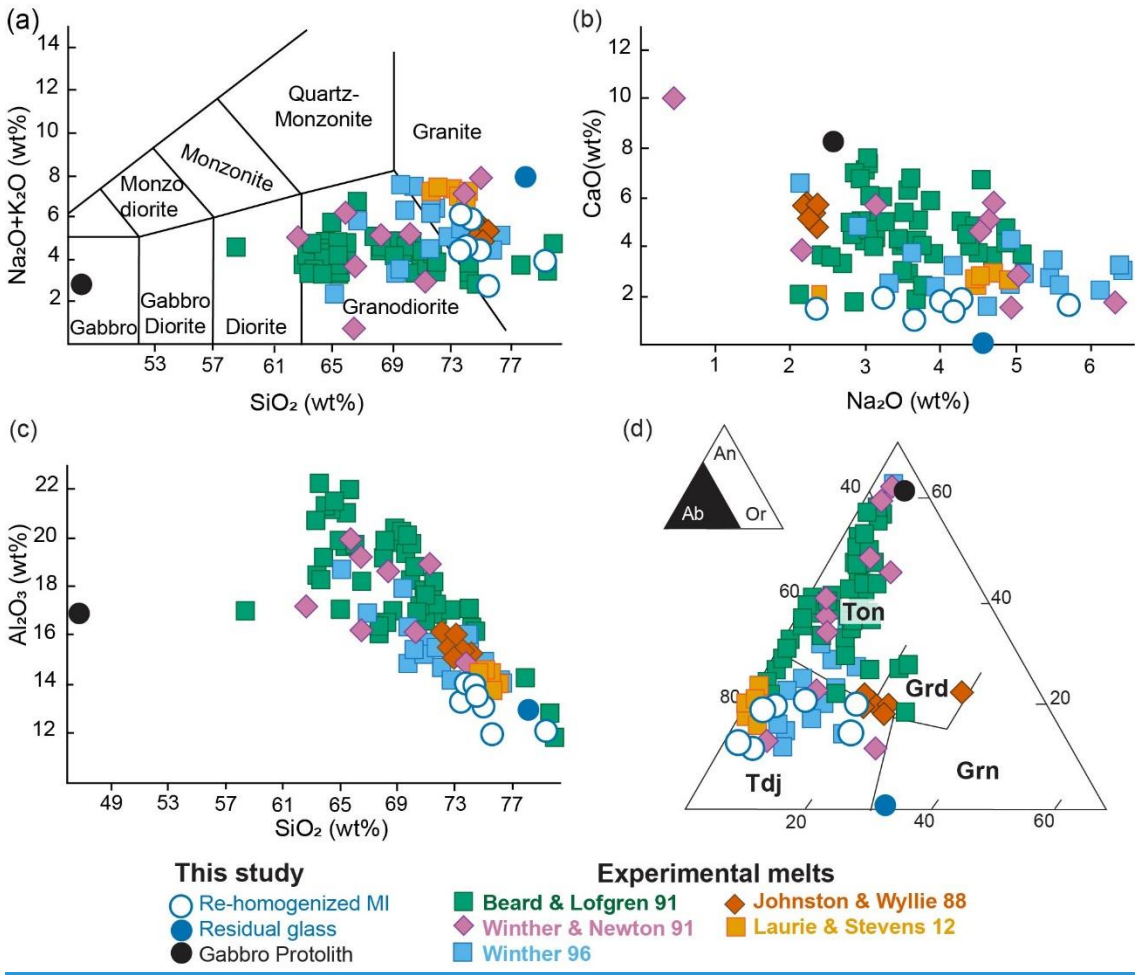

Fig. 7~~.~~: Comparison between chemical features of MI from this study and melts from experimental studies involving a mafic protolith re-melted in presence of H_2O. The entire dataset used in the figures is visible in Supplementary file Table S3. (a) TAS diagram, (b) Na_2O vs CaO plot, (c) SiO_2 vs Al_2O_3 plot ~~Molar K-Ca-Na and (b) anorthite-orthoclase-albite (An-Or-Ab) diagrams~~ and (d) Ab-Or-An ternary diagram~~showing the compositions of re-homogenized inclusions, residual glass and melts from different experimental studies involving a mafic protolith re-melted in presence of H_2O.~~ . Tdj = trondhjemite, Ton = tonalite, Grd = granodiorite and Grn = granite.

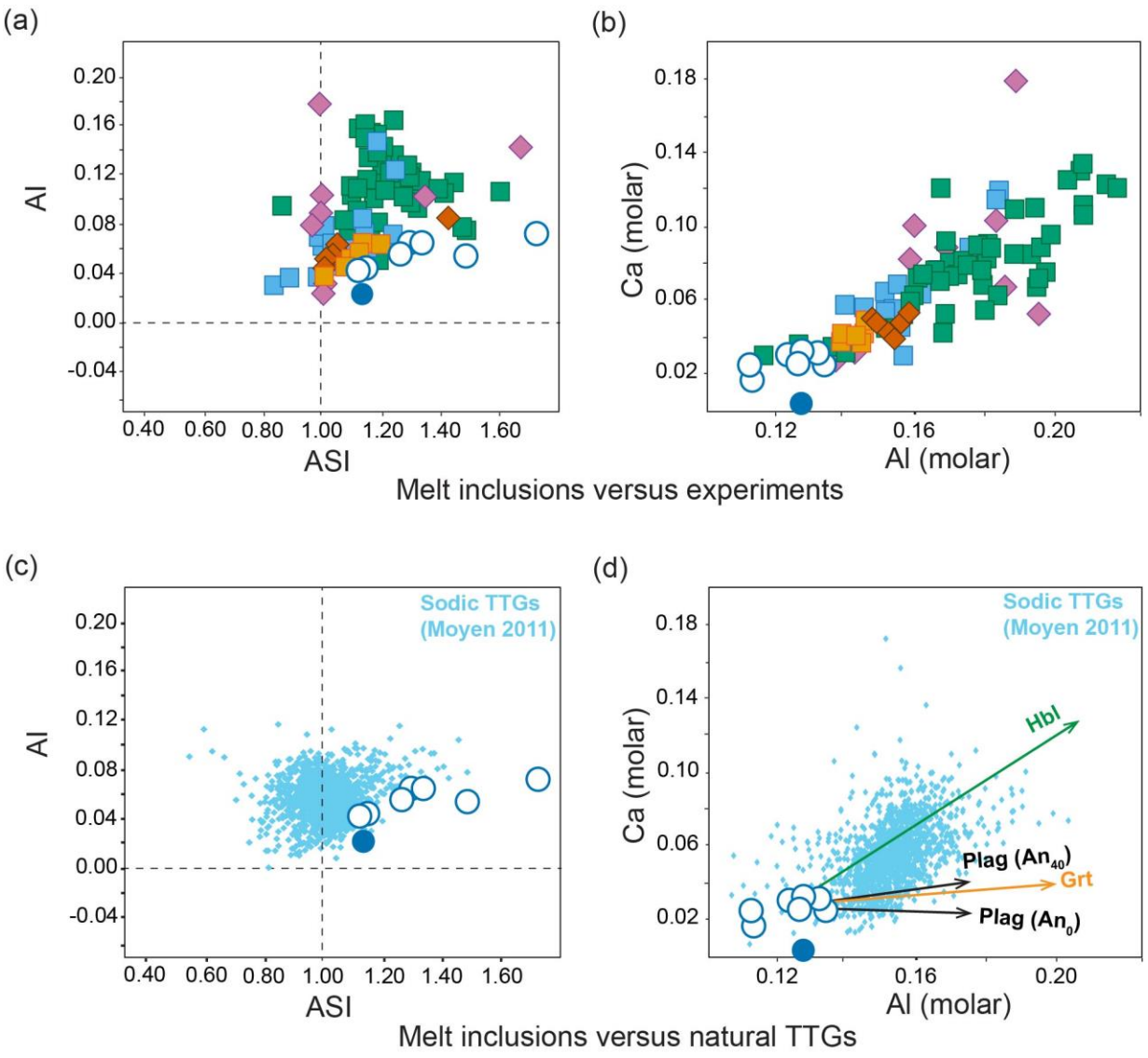

Fig. 8: ~~(c) and (e)~~ ASI vs Alkalinity Index diagrams (a, c) and ~~. (d) and (f)~~ Molar Al vs molar Ca diagrams (b, d) of Gore Mountain MI and residual glass, experimental melts and natural TTGs.~~.~~ Colors for experimental melts are defined in legend Fig. 7. Enrichment vectors are visible in (d~~f~~) pointing toward garnet (composition of megacrysts in Supplementary Table S1) and plagioclase and amphibole from Laurent et al. (2020).

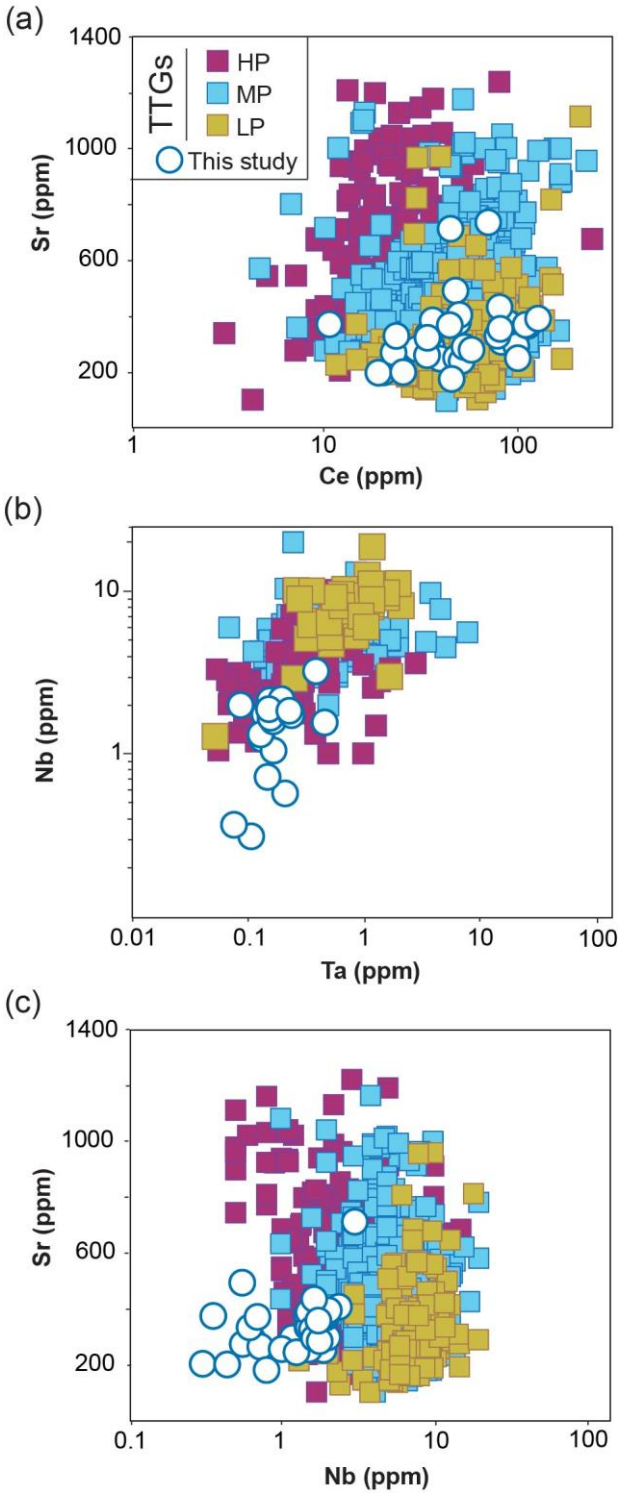

874

875 Fig. 89: Nanotrondhjemites versus TTGs. Variation diagrams of (a) Ce vs Sr, (b) Ta vs

876 Nb and (c) Nb vs Sr. Data on LP-, MP- and HP-TTGs from Moyen (2011).

Highlights

- The garnet megacrysts of Gore Mountain contain former melt inclusions
- Quartz and feldspar polymorphs commonly found as crystallization products of the trapped melt
- Melt production at ultrahigh temperature conditions (≥940°C) as result of H_2O-present partial melting of a lower crustal gabbro
- First instance of TTG embryos found in their mafic source rock
- Their mismatched chemical signature suggests that trace elements may not be diagnostic of depth of melting and geodynamic setting

Embryos of TTGs in Gore Mountain garnet megacrysts from water-fluxed melting of the lower crust

S. Ferrero[1,2], I. Wannhoff[3], O. Laurent[4,5], C. Yakymchuk[6], R. Darling[7], B. Wunder[8], A. Borghini[1] and P. O´Brien[1].

[1]*Universität Potsdam, 14476 Potsdam-Golm, Germany; sferrero@uni-potsdam.de; borghini@uni-potsdam.de; obrien@uni-potsdam.de*

[2] *Museum für Naturkunde (MfN), 10115 Berlin, Germany;*

[3] *Freie Universität Berlin, 12249 Berlin, Germany; iris.wannhoff@fu-berlin.de*

[4]*ETH, Zurich, Department Erdwissenschaften, Institute for Mineralogy and Petrology, 8092 Zürich, Switzerland*

[5]*CNRS, Observatoire Midi-Pyrénées, Géosciences Environnement, 31400 Toulouse, France; oscar.laurent@Get.omp.eu*

[6]*University of Waterloo, Waterloo, ON N2L 3G1, Canada; chris.yakymchuk@uwaterloo.ca*

[7] *SUNY College at Cortland, NY 13045,US; robert.darling@cortland.edu*

[8]*GFZ, German Research Centre for Geosciences, 14473 Potsdam, Germany; wunder@gfz-potsdam.de*

Abstract

The garnet megacrysts of Gore Mountain (Adirondacks, US) are world-renown crystals due to their size, up to 1 m in historical record, which makes them the largest known

garnets on the planet. We show here that they are also host to the first primary inclusions of trondhjemitic melt found in natural mafic rocks. The petrological and experimental investigation of the inclusions, coupled with phase equilibrium modelling, shows that this melt is the result of H_2O-fluxed partial melting at T >900°C of a lower crustal gabbro. The compositional similarity between the trondhjemitic melt inclusions and tonalitic–trondhjemitic–granodioritic (TTGs) melts makes these inclusions a direct natural evidence that melting of mafic rocks generates TTG-like melts, and provide us with the possibility to clarify processes responsible for the formation of the early continental crust. These TTG embryos represent the trondhjemitic end-member of the melts whose emplacement at upper crustal levels, after being modified by mixing and crystallization-related processes, leads to the formation of the TTG terranes. Moreover, our study shows how the melt from H_2O-fluxed melting of mafic lower crust has mismatched major and trace element signatures, previously interpreted as evidence of melting at very different pressures. This poses serious limitations to the established use of some chemical features to identify the geodynamic settings (e.g. subduction versus thickened crust) responsible for TTG generation and the growth of early crust.

1. Introduction

The garnet megacrysts of Barton mine, Gore Mountain (Adirondack Highlands, USA) are world-renowned both among petrologists and collectors for their exceptional size - 1 m crystals are recorded historically, making them some of the largest known garnets on the planet, and for their industrial use as abrasive material, with mining having occurred continuously from 1878 to 1983 (Kelly and Darling, 2008). These specimens

also display another crucial feature: the presence of silicate melt preserved as crystallized and glass-bearing inclusions of primary nature. Garnet is one of the most common and widely stable peritectic phases in metamorphic crustal rocks (Baxter et al., 2013), and it has been proven to be able to trap and preserve the melt resulting from crustal melting in more than 40 localities worldwide (Nicoli and Ferrero, 2021; Ferrero et al., 2018). Although melt inclusions (MI) are being increasingly recognized as a common feature of high-grade terranes (Bartoli and Cesare, 2020), the Gore Mountain inclusions are unique because they contain trondhjemitic melt inclusions in a mafic source rock, a feature never reported in previous studies on MI in metamorphic rocks.

Partial melting of a mafic sources has been invoked for the formation of the tonalite, trondhjemite and granodiorite (TTG) rocks, suites of sodium-rich, potassium-poor granitoids, which form the bulk of early Earth´s preserved crust (see Moyen and Martin, 2012 and references therein for a thorough review on the subject). The formation and stabilization of the earliest continental crust are key aspects of planetary evolution that can create conditions suitable for the development of complex life. Constraining the origin of TTGs is, therefore, important for models of early evolution of our planet.

Although the source rocks of TTGs are commonly inferred to be hydrated mafic rocks (Moyen and Martin, 2012), there are no known examples of melt inclusions in garnet in such metabasites. TTGs have been proposed to be generated by partial melting of subducted mafic rocks at very high pressures (HP, >2.5 GPa, Moyen, 2011) or at much shallower lower crustal conditions (<1.5 GPa) via amphibole-breakdown (Johnson et al., 2013, 2017) or water-fluxed melting (Pourteau et al., 2020). Other models propose that TTG magmas result from fractional crystallization of intermediate-mafic magmas (Jagoutz

et al., 2013; Smithies et al., 2019) possibly associated with crystal-liquid unmixing in shallow magma chambers feeding silicic eruptions (Laurent et al., 2020). The formation mechanisms of the parental TTG magmas at lower crustal depths have been investigated via geochemical and petrological characterization of TTG rocks emplaced at shallower levels (e.g. Moyen and Martin, 2012), forward modelling of putative analogues for source rocks exposed in Archean terranes (Johnson et al., 2017; Smithies et al., 2019), or using experiments (e.g. Laurie and Stevens, 2012; Qian and Hermann, 2013) and thermodynamic modelling (e.g. Kendrick and Yakymchuk, 2020).

Our finding provides a novel tool, i.e., the study of preserved MI in high-grade rocks, for the investigation of melting mechanisms in a natural mafic source region. More importantly, despite the fact that the target rocks are not Archean in age and TTG bodies are absent in the area, the similarities between the targeted MI and the TTG magmas both in terms of composition and genetic process makes of the present case study the missing link between nature, experiments and modelling results on the model of TTG petrogenesis via mafic melting.

2. Sample description

The rock investigated in this study is a garnet amphibolite of Mesoproterozoic age sampled in the pit 1 of the currently inactive mining site of Barton Mine, now Garnet Mine Tours in the Adirondacks (43°40'56"N, 74°2'51"W, Fig. 1a,b), which is an outlier of the Grenvillian orogeny (Rivers, 1997). The most apparent feature of the investigated rocks is the presence of garnet megacrysts. They form large porphyroblasts, subhedral to euhedral in shape (Fig. 1c), with size visible at the present day in the outcrop of ≤35 cm

in diameter (Kelly and Darling, 2008). Despite their size, the garnet porphyroblasts show a remarkably homogenous composition with high almandine and pyrope components and minor grossular ($Alm_{44}Prp_{42}Grs_{14}Sps_{1}$, Supplementary table S1; for details on analytical methods and techniques see the Supplementary Material). Almost every garnet is entirely surrounded by a shell of coarse-grained idiomorphic hornblende, several cm-wide (Fig. 1c). The crystallographic faces of garnet appear generally preserved at the garnet–hornblende interface at the outcrop and hand sample scale. Locally however garnet can also be surrounded by sub-millimetric symplectitic rims containing fine-grained hornblende, plagioclase, orthopyroxene and minor biotite, that formed during retrogression (mineral compositions are in Supplementary table S1; see also Hollocher, 2008). Garnet porphyroblasts and hornblende shells are hosted in a granoblastic matrix composed mainly of plagioclase and hornblende (the latter identical in major element compositions to the shell hornblende; Supplementary Table S1), plagioclase and orthopyroxene (Fig. 1c), with minor biotite and pyrite.

Previous authors generally agree that these amphibolites are the result of high-grade metamorphism during the collapse of the Ottawan orogen at 1050 Ma (e.g. McLelland and Selleck, 2011). The protolith is an olivine-bearing gabbro exposed adjacent to the amphibolites (Fig. 1b) and was originally emplaced at ~1150 Ma as part of an anorthosite-mangerite-charnockite-granite (AMCG) suite in the basement of the Adirondacks (Fig. 1a; Rivers, 1997). The extreme grain size of the rock, especially of the garnet porphyroblasts, coupled with the abundance of amphibole with respect to the gabbro protolith, has prompted several authors to propose the flux of a “copious amount of fluid” during metamorphism (McLelland and Selleck, 2011). This likely occurred along

a shear zone at the contact between gabbro and syenite (Fig. 1b), inferred to be a preferential pathway for fluid ingress (Goldblum and Hill, 1992).

3. Results

3.1 Crystallized melt inclusions

The garnet megacrysts contain a relatively large amount of polycrystalline inclusions along with crystallographically-oriented rutile needles (Fig. 2a, b). Polycrystalline inclusions are distributed as clusters in the inner portion of the garnet, which is unequivocal evidence of entrapment during garnet growth (Ferrero et al., 2018 and references therein); these inclusions are therefore primary in nature. The inclusions are aggregates of micrometric crystals in cavities of mostly isometric shape with size ≤ 50 μm across, with the smallest inclusions (<15 μm) displaying negative crystal shapes (i.e. mimicking the shape of the host garnet; Fig. 2b, c, d, e). Many inclusions have elongated tubular shapes with lengths of ≤150 μm and diameters of ≤10 μm (Fig. 1b), parallel to rutile needles. Decrepitation cracks are generally absent in the inclusions regardless their shape.

A combination of Raman spectroscopy and Field Emission Gun (FEG) electron probe microanalysis (EPMA) has shown that most of the inclusions contain an assemblage consisting of cristobalite (Fig. 2e, f; already identified by Darling et al., 1997), quartz or tridymite, plus kumdykolite (an albite polymorph; Ferrero et al., 2016) and one or both of the OH-bearing phases anthophyllite and pargasite (Fig. 2c, d, e, f). Minor amounts of phlogopite and osumilite are also present. Orthopyroxene, apatite, ilmenite and rutile needles may occur in the MI and are interpreted as trapped accessory phases,

as they are also present as mineral inclusions in the host garnet. The association of polymorphs of silica and feldspars plus OH-bearing phases is characteristic of nanogranitoids, i.e., crystallized MI in metamorphic rocks (e.g. Bartoli et al., 2016; Ferrero et al., 2018). One inclusion contains glass along with pargasite and accessory minerals; the glass is probably residual after partial crystallization of the melt originally trapped in the inclusion (Fig. 2f, g; see also glass composition in table 1). Cristobalite is present both as a crystallization product in the nanogranitoids and in association with rutile or ilmenite in a second type of polycrystalline inclusions, whose overall composition is incompatible with a former melt nature and thus will not be investigated further.

3.2 Experimental re-homogenization and melt chemistry

Multiple re-heating experiments in the temperature (T) range 900–950°C under confining pressure (P) of 1.0–1.5 GPa were performed using a piston cylinder press to re-homogenize the crystallized inclusions to glass, following the method devised by Bartoli et al. (2013; see also Supplementary Material). Experimental parameters and observations on the products of each run are listed in Fig. 3a. After the run at 900°C (experiment GM3), the inclusions show no evidence of re-melting, i.e. glass is absent. At 925°C (GM5) only the smallest inclusions (<2 μm) appear to be completely re-homogenized, whereas most inclusions contain glass in association with daughter phases such as kumdykolite and / or amphibole, and were therefore interpreted as having only undergone partial re-melting. Complete re-homogenization of the inclusions is instead common after re-heating at temperature (T) = 940°C (GM7, GM8, GM9), where nanogranitoids turn into a homogenous hydrous glass (Fig. 3b) often containing trapped

phases such as orthopyroxene (Fig. 3c), cristobalite, rutile and more rarely ilmenite (Table 1). At 950°C (GM1) the nanogranitoids are again completely re-homogenized, but cracks are common in the host and locally melt and garnet interact, which indicates disequilibrium between melt and host (Ferrero et al., 2018) and suggests that 950°C is higher than the original entrapment T of the inclusions (see discussion).

The fully re-homogenized inclusions from the experiments at 940°C were analyzed via EPMA on 7 inclusions (Fig., 4a; Table1). The resulting glass, after alkali-loss correction (see details on the procedure in Supplementary Material), is a trondhjemite with average SiO_2 = 71.89 wt%; Na_2O/CaO = 2.54 and $K_2O/Na_2O \approx 0.20$, low magnesium number (Mg# = [molar $Mg/(Mg+Fe^{2+}_{tot})$] = 0.39) and peraluminous character [Aluminium Saturation Index (ASI) = Al/(Ca+Na+K) = 1.34]. The H_2O content, measured by EMP difference, is around 4.28 wt%.

The trace element content of isometric nanogranitoids located below the surface was measured via Laser Ablation Inductively Coupled Plasma Mass Spectrometry (LA-ICP-MS) and the contribution of the host garnet subtracted after the analytical session (see methods in Supplementary Material; the whole trace element dataset is visible Table S2). Elements enriched in the host (e.g. Y, Heavy Rare Earths Elements - HREE) with respect to the inclusions are not quantifiable with this method due to the dominant signal from the host (Ferrero et al., 2018). The polycrystalline inclusions show strong enrichment in some High Field Strength Elements (HFSE), like Zr, Hf and Ti compared to the protolith gabbro (Fig. 4b), as well as enrichments of Pb, U, Th, Zn and Rare Earths elements (REE) from La to Gd (Fig. 4c). Both melt and gabbro show on average a similar positive Eu anomaly (Fig. 4c).

184

185 *3.3 Phase equilibrium modelling*

186 Phase equilibrium modelling was used to constrain independently the pressure-
187 temperature (*PT)* conditions of partial melting and peak metamorphism, as well as
188 quantify the concentration of H_2O in the system required to generate the observed mineral
189 assemblage in the garnet amphibolites of Gore Mountain. A key assumption of this
190 modelling approach is the achievement of chemical equilibrium in the system (Lanari and
191 Duesterhoeft, 2019); the macroscopic spatial distribution of garnet at the outcrop scale at
192 Gore Mountain is heterogeneous and the diffusive length scale required to maintain
193 chemical equilibrium between garnet and its matrix is unclear. Keeping this limitation in
194 mind, we use phase equilibrium modelling to provide a first-order assessment of the *P* –
195 *T* – composition *(X)* conditions required for development of the observed mineral
196 assemblages and this approach independently complements other estimates of peak
197 metamorphic conditions, such as melt re-homogenization temperatures (this study) and
198 trace element thermometry of accessory minerals (Shinevar et al., 2021). The detailed
199 modelling methods are presented in the supplementary material.

200 A temperature–composition (H_2O) phase diagram was calculated at 1.0 GPa for the
201 inferred protolith (olivine gabbro) over a range of H_2O concentrations—ranging from
202 essentially dry to H_2O-saturated at the wet solidus—to constrain the stability of the peak
203 metamorphic assemblage (garnet, hornblende, orthopyroxene, plagioclase and melt).
204 Orthopyroxene in equilibrium with anatectic melt is predicted to be stable at >800°C (Fig.
205 5a), which is a lower limit on the peak temperature. The absence of quartz from inferred
206 peak assemblage further restricts temperatures to >850°C (Fig. 5a). The modelled

concentration of H_2O in the system during the metamorphic peak (at 1.0 GPa) is restricted to <4 wt% by the presence of plagioclase and to >1 wt% H_2O by the solidus at 850°C (Fig. 5a). An additional constraint on the temperature and H_2O content of the system at peak metamorphism is provided by comparing the observed proportion of garnet in the garnet amphibolites (~13 vol.%; McLelland and Selleck, 2011) with the modelled amount (calculated as mol.% in the modelling, which is roughly equivalent to vol.% on a one-oxide molecular basis). In general, using mineral proportions is considered preferable to using mineral compositions to constrain peak *P*–*T* conditions in high-temperature metamorphic rocks (e.g. White et al., 2011). Using this approach, a modelled 13 mol.% of garnet in the system is restricted to >870°C and compositions with ~3 wt% H_2O (Fig. 5a). This indicates that the inferred peak assemblage requires substantial H_2O influx into the system when compared with the composition of the inferred protolith (~0.44 wt% H_2O, McLelland and Selleck, 2011). The temperatures of >900°C at 1.0 GPa in the model yield the observed proportion of garnet (Fig. 5a). Note that the modelled phase assemblage field that contains the observed amount of garnet is also predicted to contain a minor amount of clinopyroxene (< 8 mol.% at 1.0 GPa), which is absent from the Gore Mountain garnet amphibolites. The significance of clinopyroxene to the modelling results is discussed below.

Using the estimated 3 wt% H_2O in the system at the metamorphic peak (Fig. 5a) a pressure–temperature phase diagram was calculated to further constrain the metamorphic peak (Fig. 5b). The inferred peak metamorphic assemblage for the Gore Mountain garnet amphibolites is restricted to a small field at 810–890°C and 0.9–1.0 GPa. However, the maximum molar proportion of garnet in this field is 7 mol.%, which is roughly

half of the observed amount. To achieve a modeled 13 mol.%, garnet requires a predicted mineral assemblage with a minor amount of clinopyroxene (Fig. 5b). The modelled stability of clinopyroxene in anatectic metabasites is usually overestimated by current phase equilibrium modelling techniques. This reflects a limitation of the modelling in which the partitioning of Ca (and some other cations) between amphibole and clinopyroxene does not reproduce natural parageneses accurately (Forshaw et al., 2019). Therefore, this limitation will influence amphibole-rich rocks such as the Gore Mountain garnet amphibolites. Considering this model limitation, if we permit a small amount (< 8 mol.%) of model clinopyroxene into the peak assemblage for the investigated rocks, then the estimated peak *P*–*T* conditions are restricted to ~1.0 GPa (based on the 13 mol.% garnet isopleth) and to temperatures 850–950°C. Along the 13 mol.% garnet isopleth (Fig. 5b), the modeled amount of clinopyroxene decreases from ~8 mol.% at 950°C to ~2 mol.% at 850°C (Supplementary Fig. S1d). Therefore, we consider temperatures of >900°C permissible by the phase equilibrium modelling, with the caveat that the stability of clinopyroxene is a source of uncertainty in modelling partial melting of amphibole-rich rocks. These modelled temperatures are consistent with the temperature of MI re-homogenization (900–950°C) and yield a predicted 20–25 mol.% melt (Supplementary Fig. S1a).

4. Discussion

4.1 Silicate melt at Barton mine

Polycrystalline inclusions are present in the garnet megacrysts of Barton mine at Gore Mountain. Their phase assemblages and successful re-homogenization via experimental re-heating, coupled with the presence of preserved glass in one inclusion,

253 demonstrate that such inclusions were originally droplets of melt, now partially to totally
254 crystallized to nanogranitoids. Due to their overall trondhjemitic composition, such
255 inclusions will be hence forward called “nanotrondhjemites” in keeping with the common
256 use in nanogranitoid nomenclature (Bartoli and Cesare, 2020). A melt origin for the
257 cristobalite-bearing polycrystalline inclusions in the garnet megacrysts was already
258 proposed by Darling et al. (1997), but no melt compositions were retrieved to support this
259 hypothesis at the time. More recently, Shinevar et al. (2021) proposed the production of
260 a limited amount of melt during the formation of garnet megacrysts at Barton Mine.
261 Moreover, in the Adirondack Highlands nanogranitoids were previously reported in the
262 metapelitic gneisses of Port Leyden (Darling, 2013). Preliminary investigations also show
263 their presence also in garnets from Hooper mine (Ferrero, unpublished data), a garnet
264 mine active until 1928 (Darling, pers.comm.), suggesting that partial melting in the area
265 may be more common than previously thought.

266 Although the finding of glass-bearing nanogranitoids is a compelling evidence for
267 the (former) presence of melt in the garnet megacrysts, clear leucosome domains are not
268 conspicuous at the outcrop scale. Leucocratic pockets, several cm across in size, are
269 anyway often visible in pit 1 (Fig. 6a, b). They are mainly composed of coarse-grained
270 plagioclase ± orthopyroxene, and always closely associated with the garnet megacrysts.
271 Commonly these pockets are entirely enclosed within the amphibole shell surrounding
272 the megacrysts, making their formation likely associated to both garnet and amphibole
273 growth (Fig. 6). Such pockets could either be breakdown products of garnet with
274 contribution from the amphibole, or represent crystallized melt. The first possibility can be
275 excluded because the retrograde reaction between garnet and amphibole in these rocks

generates submillimetric symplectites of plagioclase + orthopyroxene + hornblende + biotite (Hollocher, 2008), very different both in grain size and assemblage with respect to the leucocratic pockets. This leaves only a melt-related origin for the leucocratic pockets. Hollocher (2008) ruled out also this possibility because their composition is incompatible with a melt, but this argument fails to consider that leucosome domains generally do not preserve a true melt composition due to interactions with the surrounding mineral phases, fractional crystallization and melt extraction upon cooling. These pockets may be crystallized pods of originally trondhjemitic melt now modified, a hypothesis which however requires further investigation. Regardless, such pockets would only account for ≤5 melt vol%, whereas the phase equilibria modelling predicts significantly higher melt volumes (~20–25 vol.%) to be produced at the metamorphic peak conditions (Supplementary Fig. S1). The “missing” melt (15-20 vol%) could have (re)crystallized as part of the matrix, or alternatively, left the source rock as often observed in migmatitic terranes (e.g. Brown et al., 2016). However, evidence of significant movements of melt out of the rock are absent, and indeed both garnet amphibolites and the protolith gabbro show identical bulk compositions (except for higher H_2O in the former, McLelland and Selleck, 2011), which is overall incompatible with melt loss (see also Shinevar et al., 2021).

4.2 Peculiar findings in nanotrondhjemites

The products visible in the Gore Mountain nanotrondhjemites often include unusual phases such as cristobalite, tridymite and kumdykolite and, in one case, glass. The mineral phases are polymorphs of quartz and feldspar respectively, and were already

reported in nanogranitoids hosted in rocks with widely different protoliths (from ultramafic to felsic) and partially melted under extremely variable P and T conditions, i.e., low to ultrahigh P and 700 to 1100°C (Ferrero and Angel, 2018). These phases appear to be metastable products of melt crystallization resulting from “peculiar undercooled and supersaturated conditions achieved on cooling by a melt confined in a small cavity” (Ferrero and Angel, 2018 and references therein), with crystallization kinetics of the melt likely playing a fundamental role in their formation rather than P and T conditions. Polymorphs are known to disappear, i.e. revert to their most common counterparts quartz and albite in case of inclusion reopening/decrepitation (Ferrero and Angel, 2018). Thus, their persistence in inclusions can be regarded as a strong evidence that the MI are preserved and thus the melt trapped in them maintain its original composition (Bartoli and Cesare, 2020).

Glass, visible in the present study only in one partially crystallized inclusion, is commonly observed to form in volcanic rocks as result of fast cooling: however, fully and partially crystallized MI are reported in several case studies of slowly cooled regional migmatites (Cesare et al., 2015; Ferrero et al., 2018), ruling out this possibility as the only way to create glass in natural inclusions. The presence of glass can thus be regarded as another clear evidence, besides the presence of polymorphs, that metastability may be a rather common condition attained on cooling (Ferrero and Angel, 2018) in inclusions of viscous, silica-rich melt such as the ones here investigated.

4.3 Melting at temperature in excess of 900°C in the Adirondack Highlands

The nanotrondhjemites re-homogenize completely at T ≥ 940°C and P ≥1.0 GPa, at T higher than the classic estimate of metamorphic peak T available in the Adirondack Highlands, i.e., 800-850°C and 0.65-0.86 GPa (summarized by Darling and Peck, 2016). Previous studies (Ferrero et al., 2018; 2021) have shown that the *PT* conditions at which the inclusions re-homogenize completely without evidence of decrepitation and/or melt-host interaction correspond to those of the partial melting event responsible for the formation of the inclusions (Ferrero et al., 2018 for further details). In particular, the re-homogenization T corresponds to the melting condition experienced by the rock, whereas the experimental confining P (applied to prevent MI decrepitation during re-heating) is equal to or higher with respect to the original melting P (Ferrero et al., 2018). This is also supported by a wealth of recent nanogranitoid studies where experimental *P*–*T* conditions of successful re-homogenization correspond to independently calculated partial melting conditions, e.g. classic geothermobarometry or phase equilibrium modelling (see e.g. Bartoli et al., 2013; Ferrero et al., 2018 and references therein; 2021). Thus, whereas the primary nature of the inclusions constrains the formation of garnet megacrysts at suprasolidus conditions, their re-homogenization conditions suggest ultrahigh temperature (UHT) during melting, i.e. at T in excess of 900°C. A UHT regime during garnet formation is also permissible with the results of phase equilibrium modelling (Fig. 5a, b). Phase equilibrium modelling and the similarities with previous nanogranitoid studies (Cesare et al., 2015) furthermore suggests that both melt and garnet are products of the same partial melting reaction, pointing toward a peritectic origin for the garnet megacrysts.

Although our results are at odds with the bulk of existing data on the metamorphic history of the area, we are not alone in supporting the possibility of UHT conditions in the Adirondack Highlands. Shinevar et al. (2021) provide strong mineralogical and phase equilibria evidence in support of ultrahigh T conditions (950±40°C) at Barton mine, whereas recent phase equilibrium modelling on Ledge Mountain metapelitic migmatites (30 km NNW of Barton Mine) points toward metamorphic peak conditions of >1000°C at 1.3-1.8 GPa (Davis et al., 2020). These new results call for a reappraisal of the metamorphic peak conditions experienced by the Gore Mountain garnet amphibolites and, more in general, by the rocks in the Adirondack Highlands. Further support to our interpretation that melting occurred at T >900°C is lent by the striking similarity between what we observe in the garnet amphibolites at Barton mine and the products of mafic melting experiments. A trondhjemitic melt is indeed observed to form at T >900°C at 1.3-1.5 GPa along with garnet, amphibole, plagioclase, clinopyroxene and orthopyroxene in melting experiments on starting compositions similar to the gabbro protolith inferred for the garnet amphibolites (Qian and Hermann, 2013; see also van der Laan and Wyllie, 1992). With the exception of clinopyroxene (probably also due to the slightly higher P), the experimental products correspond remarkably to the phase assemblage Grt + Hbl + Pl + Opx + Melt observed in the garnet amphibolite.

4.4 H_2O-fluxed incongruent melting in the lower crust

Incongruent melting that generates garnet in crustal rocks is generally expected to be a fluid-absent melting reaction. At Gore Mountain however the presence of a H_2O-rich fluid is necessary to explain both melt production and the extensive hornblende growth

366 (Fig. 1c) from metamorphism of a dry gabbro; moreover, garnet amphibolites have higher
367 H_2O content with respect to their gabbro protolith (see paragraph 4.1). Phase equilibrium
368 modelling of the metagabbro at 1.0 GPa demonstrates that the growth of the observed
369 ~13 vol.% peritectic garnet requires the influx of ~3 wt% H_2O at temperatures >850°C
370 (Fig. 5a, b). Thus, both modelling results and petrographic evidence point to open-system
371 conditions during melting. Our interpretation is that the main components of gabbro
372 (plagioclase, clinopyroxene, olivine) reacted with a H_2O-rich fluid to produce the
373 assemblage visible in the garnet amphibolite (i.e., garnet, amphibole, plagioclase,
374 orthopyroxene and melt), which also corresponds to the (near?) peak metamorphic
375 assemblage visible in Fig. 5. Both presence of MI in the inner portion of garnet megacrysts
376 and the lack of prograde zoning (Hollocher, 2008) support garnet growth entirely at (or
377 close to) metamorphic peak conditions, i.e., at >900°C and ~1.0 GPa.

378 The trace element content of the melt resembles that of the gabbro, confirming the
379 latter as the melt source. The most notable geochemical feature of the melt is the strong
380 enrichment in Th, U and some High Field Strength Elements (HFSE), like Zr, Hf and Ti
381 compared to the source gabbro (Fig. 4b). At high T and lower crustal conditions,
382 especially in presence of Na and Si (Mysen, 2015 and references therein), HFSE, U and
383 Th can be transported in H_2O-rich fluids and subsequently transferred into the melt
384 (Borghini et al., 2020). The melt shows a high concentration of Zr (1400 ppm average),
385 twice the expected amount (~690 ppm) based on zircon solubility (Boehnke et al., 2013)
386 at the corresponding temperature and inferred major-element melt composition.
387 Inclusions of zircon (typical host of Zr and Hf) are very rare in Gore Mountain MI, and
388 zircon-bearing inclusions were carefully avoided during analyses. This suggests that both

Zr and Hf enrichments are features of the melt itself, likely related to the increase in HFSE solubility in the presence of a free fluid (Bartels et al., 2010). Nb and Ta should be equally transported in the kind of fluid discussed here, but they are yet not as enriched as Zr-Hf-Th-U in the melt inclusions. This could be due to the growth of ilmenite (and possibly even rutile), observed as mineral inclusions in garnet, during metamorphism and melting and likely to contain a sizable amount of Nb and Ta.

In presence of an infiltrating fluid, the melt would be furthermore expected to be enriched in Large Ion Lithophile Elements (LILEs), incompatible components generally partitioned in fluids (Cannaó and Malaspina, 2018). However, in our case study LILE and HFSE appear to be decoupled, i.e., the melt shows no particular enrichment in Cs, Rb, Ba and Sr relative to the host gabbro (Fig. 4b). This may suggest a LILE-poor source, e.g. possibly related to the mantle rather than to the crust. Finally, also the H_2O-rich nature of the fluid itself is unexpected in the lower portion of an orogen undergoing collapse at the time of garnet megacrysts formation (1050 Ma; see McLelland and Selleck, 2011). The enigma represented by the fluid origin requires further studies, currently underway and involving stable isotopes investigation (Ferrero et al., in preparation).

Although the presence of a free fluid during melting of the mafic lower crust (at $P \geq 1.0$ GPa) was not regarded as a common situation (Moyen and Martin, 2012), this has been recently proposed to explain the origin of arc granitoids and the continental crust in general (Collins et al., 2020; Pourteau et al., 2020). In the case of Gore Mountain, Goldblum and Hill (1992) suggested that the high ductility contrast between the original gabbro and the surrounding metasyenites caused the formation of a shear zone (Fig. 1b), which acted as preferential pathway for the ingress of fluid at depth.

In summary, we propose that the olivine gabbro, prior to fluid infiltration, resided in the lower part of the orogen at T in excess of 900°C without undergoing melting because of its very dry composition (0.44 wt% H_2O, McLelland and Selleck, 2011) and elevated solidus temperature, e.g. >1000°C for this H_2O content (dashed line in Fig. 5a). The infiltration of a H_2O-rich fluid decreased significantly the solidus of the gabbro assemblage, allowing its mineral components to undergo melting, as a response to the change in H_2O content in the system. This may have taken place either at the same PT conditions present before melting or during an increase of both P and T, as recently proposed by Shinevar et al. (2021).

4.5 Nanotrondhjemites, experimental melts and natural TTGs

The trondhjemitic melt enclosed in the nanogranitoids of Gore Mountain is hydrous, peraluminous and with very low maficity (Table 1). The high ASI of the melt preserved at Gore Mountain cannot be ascribed to interaction with the host garnet, as evidence of chemical interaction, either chemical zoning in the garnet surrounding the re-homogenized inclusions or embayments in the inclusion walls (see paragraph 4.2), are completely absent in the analyzed inclusions. The peraluminous character is consistent with the presence of osumilite as minor daughter phase in the inclusions: this phase is a rare alumina-rich, double-ring silicate found both in igneous and metamorphic UHT rocks (Kelsey, 2008). An oddity is however the presence of amphibole as daughter mineral in the inclusions: these phases are indeed more common in metaluminous rather than peraluminous melts (Bonin et al., 2020 and references therein), and this remains an enigmatic aspect of these nanotrondhjemites.

Nanogranitoids are natural capsules where melt is trapped immediately after production and then preserved (Cesare et al., 2015), making them directly comparable to melts from mafic melting experiments in presence of H_2O (Fig. 7). The re-homogenized inclusions plot in the granitic field of the total alkali versus silica (TAS) diagram (Fig. 7a), near the most silica-rich experimental melts (e.g., Laurie and Stevens, 2012). The inclusions show a range of Na_2O values consistent with the experimental dataset on mafic melting, whereas both CaO (Fig. 7b) and Al_2O_3 (Fig. 7c) are generally lower than the majority of the experimental melts, in agreement with the trondhjemitic nature of the inclusions (see also the Ab-Or-An ternary diagram, Fig. 7d). In general, the trapped melt appears to be lower in alkalis than most experimental melts even after alkali-correction, a feature likely to contribute to the high ASI displayed by these melts (Fig. 8a), despite the generally low Al content of the inclusions (Figs. 8b; 7c). Moreover, the investigated nanotrondhjemites appear to represent the low-calcium, low-alumina “end-member” of the positive trend defined by the cloud of experimental melts (Fig. 8b). The observed chemical differences could be explained by slightly different starting compositions. The Gore Mountain gabbro has a peculiar composition and is notably more mafic and showing higher Al/Ca ratio than all the starting materials from mafic melting experiments compiled here (1.13 vs. 0.63-1.01; all values are reported in Supplementary Table S4). In fact, as part of an anorthosite suite (McLelland and Selleck, 2011), it somewhat differs in composition from expected sources for TTGs that are rather tholeiitic to transitional basalts / amphibolites (Moyen and Martin, 2012). Despite these differences, the range of ASI values found in the nanotrondhjemites is fully comparable to the experimental melts

457 (Fig. 8a), indicating that the Al_2O_3, CaO, Na_2O and K_2O balance is consistent with phase
458 relations characterizing the melting of mafic rocks.

459 When compared to natural TTGs, the Gore Mountain MI display higher ASI and
460 similar AI (Fig. 8c) and both lower Ca and Al (Fig. 8d). A discrepancy is however not
461 unexpected: as mentioned above, the source composition of the Gore Mountain MI might
462 not be a perfect match to that of TTG magmas. In addition, these nanogranitoids contain
463 a pristine melt trapped directly at the source region, making them necessarily different
464 from TTG plutons/complexes, whose compositional diversity results from processes
465 occurring in the source, during magma ascent and during emplacement. Mixing of melts
466 from different sources and entrainment of residual or peritectic material is also recognized
467 to increase the compositional scatter of crustal melts with respect to their starting
468 composition measured in nanogranitoids from more felsic rocks (Bartoli et al, 2016).
469 Moreover, magma differentiation (Smithies et al., 2019) and crystal-liquid separation
470 during emplacement in the upper crust (Laurent et al., 2020) were recently proposed to
471 be influential factors in shaping TTG geochemistry. In particular, the rocks composing
472 some upper crustal TTG plutons (diorites, tonalites, trondhjemites) may represent
473 plagioclase ± amphibole cumulates instead of true liquid compositions (Laurent et al.,
474 2020). In fact, the Ca vs. Al compositional variability of natural TTGs is well encompassed
475 by considering mixing in various proportions between a liquid similar to the Gore Mountain
476 inclusions and these two minerals (Fig. 8d). This model also explains the lower Si, mafic
477 elements and higher Na concentrations of natural trondhjemites (presumably plagioclase
478 cumulates) than the Gore Mountain nanotrondhjemites (inferred primary liquids). In this
479 perspective, the Gore Mountain MI are “embryos” (Bartoli et al., 2014) of TTGs, in the

same way that nanogranitoids in silica-rich crustal rocks are embryos of S-type granites (Bartoli et al., 2016).

4.6 Implications for TTG petrogenesis

Although the composition of the Gore Mountain and natural TTGs may not be directly comparable in details, both bear a typical geochemical signature resulting from melting of K-poor mafic rocks, i.e., their silica-rich, trondhjemitic signature. Therefore, both can be discussed together to better constrain such melting processes, relevant to the generation of the Earth's earliest continental crust. In studies based on natural samples, this signature is interpreted to result from melting at P ≥2.0 GPa in equilibrium with garnet and rutile, defining the so-called "High-Pressure" TTG (HP-TTG) group (Moyen, 2011). Thermodynamic modelling on Archean mafic rocks have recently shown that HP-TTGs may form at 900-950°C and lower P, i.e. 1.3-1.8 GPa (Kendrick and Yakymchuk, 2020) and down to 1.2 GPa (Johnson et al., 2017). Our finding shows that it is possible to form trondhjemitic melts with broadly comparable major elements signatures with HP-TTGs at similar T (≥ 925°C) and P conditions (1.0 GPa), directly from melting of lower crustal mafic rocks. Moreover, the Gore Mountain garnet amphibolite displays all the mineralogical hallmarks characteristic of residues of "low-pressure" (LP-) TTGs (i.e. formed at < 1.2 GPa, Moyen, 2011): amphibole and plagioclase are abundant, and orthopyroxene is present instead of clinopyroxene. This apparent discrepancy between melt and residual compositions may result from a significantly different melting process than generally assumed. Although the source system is dominated by LP assemblages, the liquid itself is in equilibrium with a solid assemblage containing phases more characteristic of much

503 deeper melting, i.e. garnet and rutile. This reflects the incongruent melting of mafic rocks,
504 with garnet and rutile production as melting initiates, whereas this has been regarded so
505 far in TTG petrogenesis as a mainly eutectic process, with garnet and other components
506 of the residue being already present before the initiation of melting, and then in excess
507 during melting (Moyen and Martin, 2012). However, the absence of relicts of sub-solidus
508 portions in the garnet megacrysts, i.e., a clear prograde zoning, despite its pluri-
509 decimetric size supports the evidence that these porphyroblasts started growing only at
510 the onset of the melting, similarly to what was observed in experiments on mafic rocks
511 (Beard and Lofgren, 1991) and other systems (Patiño Douce and Harris, 1998).

512 Conversely, the trace element concentrations of Gore Mountain MI show contrasting
513 LP-like and HP-like features. Sr and LREE contents are fully compatible with LP-TTGs
514 (Fig. 9a), whereas Nb and Ta are very low, as typically ascribed to HP-TTGs (Fig. 9b, c)
515 due to the presence of rutile and ilmenite as well as amphibole (for Nb) in the residue.
516 Thermodynamic calculations on Archean basalts (Johnson et al., 2017) have shown that
517 TTGs with garnet + rutile residue may indeed form at P as low as 1.2 GPa, typical of LP-
518 TTGs, thus supporting the idea that LP melts from mafic melting can share features with
519 HP-TTGs. This requires a careful re-evaluation of the existent databases, insofar as some
520 TTGs currently classified as HP-TTGs based on Nb and Ta contents should be instead
521 classified as LP-TTGs.

522

523 **5. Conclusions**

524 The garnet megacrysts of Barton mine at Gore Mountain have been attracting the
525 attention of expert scientific audience and general public alike since their discovery in the

526 1850's (Kelly and Darling, 2008) because of their unparalleled size. This feature swayed
527 the attention of most of the scientific community toward the macroscale features of these
528 crystals, at the expenses of high-resolution studies in the garnet interiors (with the
529 remarkable exception of Shinevar et al. 2021). Our work shows how novel insights into
530 geological processes with both local and worldwide relevance can be gained from the
531 study of the microstructural features of such rocks. Our petrographic, experimental and
532 modelling results prove for the first time that these garnets are peritectic and preserve
533 micrometric droplets of trondhjemitic melt. Such melt results from the H_2O-fluxed melting
534 of a gabbro in the lower crust during ultrahigh temperature metamorphism, a condition
535 only recently recognized in the Adirondack Highlands (Shinevar et al., 2021) and still
536 controversial. Further studies are needed to relate our solid microstructural and
537 microchemical constraints to the geodynamic evolution of the area during the late
538 Mesoproterozoic.

539 The compositional similarity between the trondhjemitic MI and TTGs provides us
540 with the possibility to directly investigate the composition of the trondhjemitic melt, the
541 phases coexistent with it as well as its mafic source rock, generated under well-
542 constrained conditions. Our work shows how H_2O-fluxed partial melting of mafic crust
543 creates TTG-like melts with "HP-like" major elements and hybrid traces, i.e., "LP-like" in
544 Sr and Ce contents and "HP-like" in Nb and Ta. Previously thought to be smoking guns
545 of different melting P (at crustal versus mantle depths), such contrasting features within
546 a single melt inclusion demonstrates that trace element signatures of TTGs are not
547 diagnostic of depth of melting and geodynamic setting (see also Smithies et al., 2019).
548 This result is complementary to recent findings that crystal-liquid segregation in TTG

plutons can result in similar discrepancies (Laurent et al., 2020), pointing out that both source processes (melting reaction, H_2O activity) and magma chamber dynamics exert a first-order control on TTG geochemistry, instead of melting pressure. Our finding provides support to the idea of a two-stage mechanism of TTG production (Moyen and Martin, 2012), i.e., mantle melting to produce basalt/gabbro, followed by melting of basalt/gabbro at lower crustal conditions to produce the TTG parental magma. This does not invalidate however other TTG production models, i.e. a one-stage mechanism whereby TTGs are produced by direct fractional crystallization of hydrous basalts (Jagoutz et al., 2013), which remain a valid explanation for occurrences where TTG granitoids are associated with magmatic cumulates in the lower crust.

In conclusion, these TTG embryos are a direct natural evidence that melting of mafic rocks generates TTG-like melts, in agreement with previous research (e.g., Johnson et al., 2012; Porteau et al., 2020), and that such melts can be found in the source region as MI. It is arguable that the production of TTG-like melts at Gore Mountain is the result of a peculiar set of circumstance of local significance, i.e., local H_2O-rich fluid infiltration at depth. Nevertheless, H_2O-fluxed melting of lower crustal mafic rocks is increasingly recognized as a fundamental process for the production of TTGs, thus lending to our findings a clear and undoubtable relevance for the advancement of our understanding of TTG petrogenesis.

Acknowledgements

Our deepest thanks go to Bonnie Barton for being an outstanding guide during our visit to Barton Mines. The present research was funded by the German Federal Ministry for

572 Education and Research and the Deutsche Forschungsgemeinschaft (Project FE 1527/2-
573 2) to SF. We are grateful to C. Günter, M.A. Ziemann, F. Wilke, F. Kaufmann and L. Hecht
574 for help during analyses and to C. Fischer for sample preparation. The comments of T.
575 Tacchetto and other anonymous reviewers on an earlier (shorter) version, and of O.
576 Jagoutz and T. Johnson on the latest version led to an improvement in both clarity and
577 significance of the present manuscript.
578
579 *References*
580 Bartels, A., Holtz, F., and Linnen, R. L., 2010, Solubility of manganotantalite and
581 manganocolumbite in pegmatitic melts: American Mineralogist, v. 95 (4), p. 537-
582 544, https://doi.org/10.2138/am.2010.3157.

583 Bartoli, O., Cesare, B., Poli, S., Acosta-Vigil, A., Esposito, R., Turina, A., Bodnar, R.
584 J., Angel, R. J., and Hunter, J., 2013, Nanogranite inclusions in migmatitic garnet:
585 behavior during piston-cylinder remelting experiments: Geofluids, 13, p. 405-420,
586 https://doi.org/10.1111/gfl.12038.

587 Bartoli, O., Cesare, B., Remusat, L., Acosta-Vigil, A., and Poli, S, 2014, The H_2O
588 content of granite embryos: Earth and Planetary Science Letters, v. 395, p. 281–
589 290, https://doi.org/10.1016/j.epsl.2014.03.031.

590 Bartoli, O., Acosta-Vigil, A., Ferrero, S., and Cesare, B., 2016, Granitoid magmas
591 preserved as melt inclusions in high-grade metamorphic rocks: American
592 Mineralogist, v. 101, p. 1543–1559, https://doi.org/10.2138/am-2016-
593 5541CCBYNCND.

Bartoli, O., and Cesare, B., 2020. Nanorocks: a 10 year old story: Rendiconti Lincei. Scienze Fisiche e Naturali, v. 31, p. 249-257, https://doi.org/10.1007/s12210-020-00898-7.

Baxter, E. F., Caddick, M. J., and Ague, J. J., 2013, Garnet: Common mineral, uncommonly useful. Elements, v. 9(6), p. 415-419.

Beard, J. S., and Lofgren, G. E., 1991, Dehydration melting and water-saturated melting of basaltic and andesitic greenstones and amphibolites at 1, 3, and 6. 9 kb: Journal of Petrology, v. 32, p. 365-401, https://doi.org/10.1093/petrology/32.2.365.

Boehnke, P., Watson, B. E., Trail, D., Harrison, T. M., and Schmitt, A. K., 2013, Zircon saturation re-revisited: Chemical Geology, v. 351, p. 324–334, https://doi.org/10.1016/j.chemgeo.2013.05.028.

Bonin, B., Janoušek, V., and Moyen, J.-F:, 2020, Chemical variation, modal composition and classification pf granitoids, *in* Janoušek, V., Bonin, B., Collins, W.J., Farina, F., and Bowden, P., eds., Post-Archean Granitic Rocks: Petrogenetic Processes and Tectonic Environments: Geological Society, London, Special Publications, v. 491, p. 9-51, https://doi.org/10.1144/SP491-2019-138.

Borghini, A., Ferrero, S., O'Brien, P. J., Laurent, O., Günter, C., and Ziemann, M. A., 2020, Cryptic metasomatic agent measured in situ in Variscan mantle rocks: Melt inclusions in garnet of eclogite, Granulitgebirge, Germany: Journal of Metamorphic Geology, v. 38, p. 207–234, https://doi.org/10.1111/jmg.12519.

615 Brown, C. R., Yakymchuk, C., Brown, M., Fanning, C. M., Korhonen, F. J., Piccoli, P.
616 M., and Siddoway, 2016, From Source to Sink: Petrogenesis of Cretaceous
617 Anatectic Granites from the Fosdick Migmatite – Granite Complex, West
618 Antarctica: Journal of Petrology, v. 57 (7), p. 1241-1278,
619 https://doi.org/10.1093/petrology/egw039.

620 Cannaó, E., and Malaspina, N., 2018, From oceanic to continental subduction:
621 Implications for the geochemical and redox evolution of the supra-subduction
622 mantle: Geosphere, v. 14, no. 6, p. 2311-2336, https:// doi .org /10 .1130
623 /GES01597 .1.

624 Cesare, B., Acosta-Vigil, A., Bartoli, O., and Ferrero, S., 2015, What can we learn from
625 melt inclusions in migmatites and granulites? Lithos, v. 239, p. 186-216,
626 https://doi.org/10.1016/j.lithos.2015.09.028.

627 Collins, W. J., Murphy, J. B., Johnson, T. E., and Huang, H.-Q., 2020, Critical role of
628 water in the formation of continental crust: Nature Geoscience, v. 13, p. 331-338,
629 https://doi.org/10.1038/s41561-020-0573-6.

630 Darling, R. S., 2013, Zircon-bearing, crystallized melt inclusions in peritectic garnet
631 from the western Adirondack Mountains, New York State, USA: Geofluids, v. 13
632 (4), p. 453-459, https://doi.org/10.1111/gfl.12047.

633 Darling, R. S., Chou, I.-M., and Bodnar, R. J., 1997, An occurrence of metastable
634 cristobalite in high-pressure garnet granulite: Science, v. 276, p. 91–93,
635 https://doi.org/10.1126/science.276.5309.91.

636 Darling, R.S. and Peck, W.H., 2016, Metamorphic conditions of Adirondack rocks:
637 Adirondack Journal of Environmental Studies, v. 21, Article 7.

638 Davis, M., Leech, M. and Metzger, E.P., 2020, Determining the Petrotectonic
639 Evolution of Ledge Mountain Migmatites with Phase Equilibria Modelling and Melt
640 Reintegration: Adirondack Highlands, New York. Abstract V019-0004 presented at
641 2020 Fall Meeting, AGU, San Francisco, CA, 1-17 Dec.

642 Ferrero, S., and Angel, R. J., 2018, Micropetrology: are inclusions in minerals grains
643 of truth? Journal of Petrology, v. 59, p. 1671–1700, doi: 10.1093/petrology/egy075.

644 Ferrero, S., O'Brien, P. J., Borghini, A., Wunder, B., Wälle, M., Günter, C., and
645 Ziemann, M. A., 2018, A treasure chest full of nanogranitoids: an archive to
646 investigate crustal melting in the Bohemian Massif, *in* Ferrero, S., Lanari, P.,
647 Goncalves, P., and Grosch, E. G., eds., Metamorphic Geology: Microscale to
648 Mountain Belts: Geological Society, London, Special Publications 478, p. 13-38,
649 https://doi.org/10.1144/SP478.19.

650 Ferrero, S., Ague, J.J., O'Brien, P.J., Wunder, B., Remusat, L., Ziemann, M.A., Axler,
651 J., 2021, High pressure, halogen-bearing melt preserved in ultra-high temperature
652 felsic granulites of the Central Maine Terrane, Connecticut (US): American
653 Mineralogist, in press, https://doi.org/10.2138/am-2021-7690.

654 Forshaw, J. B., Waters, D. J., Pattison, D. R. M., Pallin, R., and Gopon, P., 2019, A
655 comparison of observed and thermodynamically predicted phase equilibria and
656 mineral compositions in mafic granulites: Journal of Metamorphic Geology, v. 37,
657 p. 153-179, https://doi.org/10.1111/jmg.12454.

Goldblum, D. R., and Hill, M. L., 1992, Enhanced fluid flow resulting from competency contrast within a shear zone: The garnet ore zone at Gore Mountain, N.Y: The Journal of Geology, v. 100, p. 776–782, https://doi.org/10.1086/629628.

Hollocher, K., 2008, Origin of big garnets in amphibolites during high-grade metamorphism, Adirondacks, New York: 21st Annual Keck Undergraduate Research Symposium, p. 129–134.

Jagoutz, O., Schmidt, M. W., Enggist, A., Burg, J.-P., Hamid, D., and Hussain, S., 2013, TTG-type plutonic rocks formed in a modern arc batholith by hydrous fractionation in the lower arc crust: Contributions to Mineralogy and Petrology, v. 166(4), p. 1099-1118, https://doi.org/10.1007/s00410-013-0911-4.

Johnson, T. E., Brown, M., Kaus, B. J. P., and VanTongeren, J. A., 2013, Delamination and recycling of Archaean crust caused by gravitational instabilities: Nature Geoscience, v. 7, p. 47–52, https://doi.org/10.1038/ngeo2019.

Johnson, T. E., Brown, M., Gardiner, N. J., Kirkland, C. L., and Smithies, R. H., 2017, Earth's first stable continents did not form by subduction: Nature, v. 543, p. 239–242, https://doi.org/10.1038/nature21383.

Johnson, T. E., Fischer, S., White, Brown, M., Rollinson, H.R., 2012, Archaean intracrustal differentiation from partial melting of metagabbro—field and geochemical evidence from the central region of the Lewisian complex, NW Scotland: Journal of Petrology, v. 53 (10), p. 2115–2138. https://doi.org/10.1093/petrology/egs046

679 Johnston, A. D., and Wyllie, P. J., 1988, Constraints on the origin of Archean
680 trondhjemites based on phase relationships of Nûk gneiss with H_2O at 15 kbar:
681 Contributions to Mineralogy and Petrology, v. 100, p. 35-46,
682 https://doi.org/10.1007/BF00399438.

683 Kelly, W.M., and Darling, R. S., 2008, Geology and mining history of the Barton garnet
684 mine, Gore Mt., and the NL ilmenite mine, Tahawus, NY with a temporal excursion
685 to the Macintyre, *in* Selleck, B.W., 80th Annual Meeting of the New York State
686 Geological Association, Fieldtrip Guidebook, 154 p.

687 Kelsey, D. E., 2008, On ultrahigh-temperature crustal metamorphism: Gondwana
688 Research, v. 13 (1), p. 1-29, https://doi.org/10.1016/j.gr.2007.06.001.

689 Kendrick, J., and Yakymchuk, C., 2020, Garnet fractionation, progressive melt loss
690 and bulk composition variations in anatectic metabasites: Complications for
691 interpreting the geodynamic significance of TTGs: Geoscience Frontiers, v. 11, p.
692 745-763, https://doi.org/10.1016/j.gsf.2019.12.001.

693 Lanari, P. and Duesterhoeft, E., 2019, Modelling metamorphic rocks using equilibrium
694 thermodynamics and internally consistent databases: past achievements, problems
695 and perspectives: Journal of Petrology, 60(1), p.19-56,
696 https://doi.org/10.1093/petrology/egy105.

697 Laurent, O., Björnsen, J., Wotzlaw, J.-F., Bretscher, S., Pimenta Silva, M., Moyen, J.-
698 F., Ulmer, P., and Bachmann, O., 2020, Earth's earliest granitoids are crystal-rich
699 magma reservoirs tapped by silicic eruptions: Nature Geoscience, v. 13(2), p. 163-
700 169, https://doi.org/10.1038/s41561-019-0520-6.

Laurie, A., and Stevens, G., 2012, Water-present eclogite melting to produce Earth's early felsic crust: Chemical Geology, v. 314–317, p. 83–95, https://doi.org/10.1016/j.chemgeo.2012.05.001.

McLelland, J. M., and Selleck, B. W., 2011, Megacrystic Gore Mountain–type garnets in the Adirondack Highlands: Age, origin, and tectonic implications: Geosphere, v. 7, p. 1194–1208, https://doi.org/10.1130/GES00683.1.

Moyen, J.-F., 2011, The composite Archaean grey gneisses: Petrological significance, and evidence for a non-unique tectonic setting for Archaean crustal growth: Lithos, v. 123(1-4), p. 21-36, https://doi.org/10.1016/j.lithos.2010.09.015.

Moyen, J.-F., and Martin, H., 2012, Forty years of TTG research: Lithos, v. 148, p. 312–336, https://doi.org/10.1016/j.lithos.2012.06.010.

Mysen, B., 2015, An in situ experimental study of Zr^{4+} transport capacity of water-rich fluids in the temperature and pressure range of the deep crust and upper mantle: Progress in Earth and Planetary Science, v. 2, 38, https://doi.org/10.1186/s40645-015-0070-5.

Nicoli, G., and Ferrero, S., 2021, Nanorocks, volatiles and plate tectonics: Geoscience Frontiers, accepted.

Patiño Douce, A. E., and Harris, N., 1998, Experimental constraints on Himalayan anataxis: Journal of Petrology, v. 39(4), p. 689-710, https://doi.org/10.1093/petroj/39.4.689.

721 Pourteau, A., Ducet, L. S., Blereau, E. R., Volante, S., Johnson, T. E., Collins, W. J.,
722 Li, Z.-X., and Champion, D. C., 2020, TTG generation by fluid-fluxed crustal
723 melting: Direct evidence from the Proterozoic Georgetown Inlier, NE Australia, v.
724 550, https://doi.org/10.1016/j.epsl.2020.116548.

725 Qian, Q., and Hermann, J., 2013, Partial melting of lower crust at 10–15 kbar:
726 constraints on adakite and TTG formation: Contributions of Mineralogy and
727 Petrology, v. 165, p. 1195–1224, https://doi.org/10.1007/s00410-013-0854-9.

728 Rivers, T., 1997, Lithotectonic elements of the Grenville Province: review and tectonic
729 implications: Precambrian Research, v. 167, p. 117-154,
730 https://doi.org/10.1016/S0301-9268(97)00038-7.

731 Shinevar, W.J., Jagoutz, O., and VanTongeren, J.A., 2021, Gore Mountain Garnet
732 Amphibolite records UHT Conditions: Implications for the Rheology of the Lower
733 Continental Crust During Orogenesis: Journal of Petrology, accepted,
734 https://doi.org/10.1093/petrology/egab007.

735 Smithies, R. H., Lu, Y., Johnson, T., Kirkland, C. L., Cassidy, K. F., Champion, D. C.,
736 Mole, D. R., Zibra, I., Gessner, K., Sapkota, J., De Paoli, M. C., and Poujol, M.,
737 2019, No evidence for high-pressure melting of Earth's crust in the Archean:
738 Nature Communications, v. 10, 5559, https://doi.org/10.1038/s41467-019-13547-
739 x.

740 van der Laan, S. R., and Wyllie, P. J., 1992, Constraints on Archean Trondhjemite
741 Genesis from Hydrous Crystallization Experiments on Nûk Gneiss at 10-17 kbar:
742 The Journal of Geology, v. 100, p. 57-68.

White, R.W., Stevens, G. and Johnson, T.E., 2011. Is the crucible reproducible? Reconciling melting experiments with thermodynamic calculations. Elements, 7(4), p. 241-246.

Winther, T. K., 1996, An experimentally based model for the origin of tonalitic and trondhjemitic melts: Chemical Geology, v. 127, p. 43–59, https://doi.org/10.1016/0009-2541(95)00087-9.

Winther, T. K., and Newton, R. C., 1991, Experimental melting of a hydrous low-K tholeiite: evidence on the origin of Archaean cratons: Bulletin of the Geological Society of Denmark, v. 39.

Captions

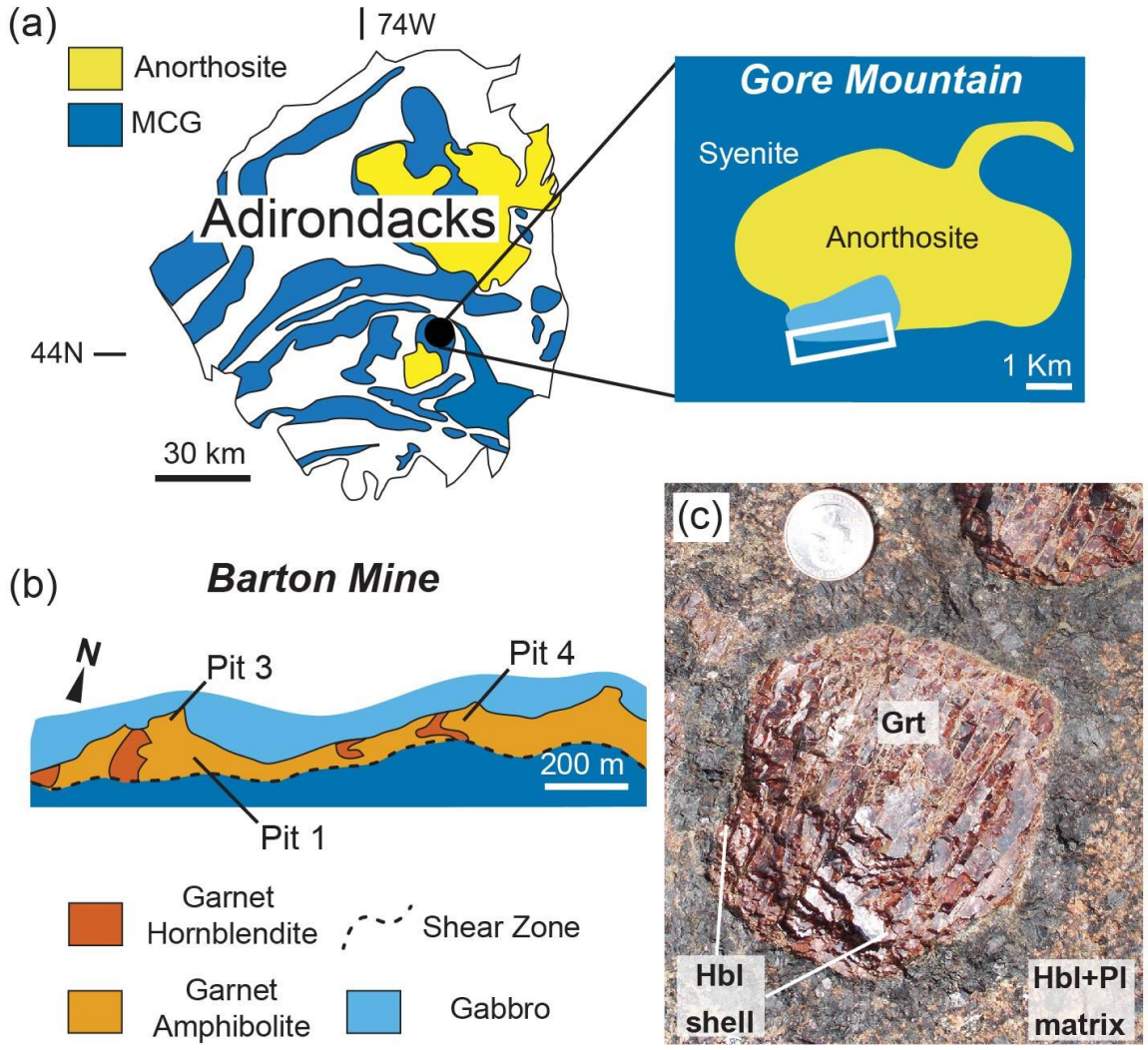

Fig. 1. a) Simplified geological setting (modified after McLelland and Selleck, 2011) of the Adirondacks (NY state, US) showing the rock types of interest. MCG= mangerite-charnockite-granite suite. Black dot= location of Gore Mountain, with general geologic setting in the inset on the right. White box= location of Barton Mine. (b) Detailed geological map of the open pit of Barton Mine. The inclusion-bearing garnets investigated in this study are from the garnet amphibolites; the garnet hornblendites present along with the amphibolites have smaller garnets hosted in a matrix of pluri-cm hornblende, and were

not investigated in the present study. The location of the shear zone is based on Goldblum and Hill (1992). (c) Garnet (Grt) megacryst surrounded by hornblende (Hbl) in a matrix of Hbl and plagioclase (Pl) and minor orthopyroxene, not visible in the figure. Coin diameter= 2.5 cm.

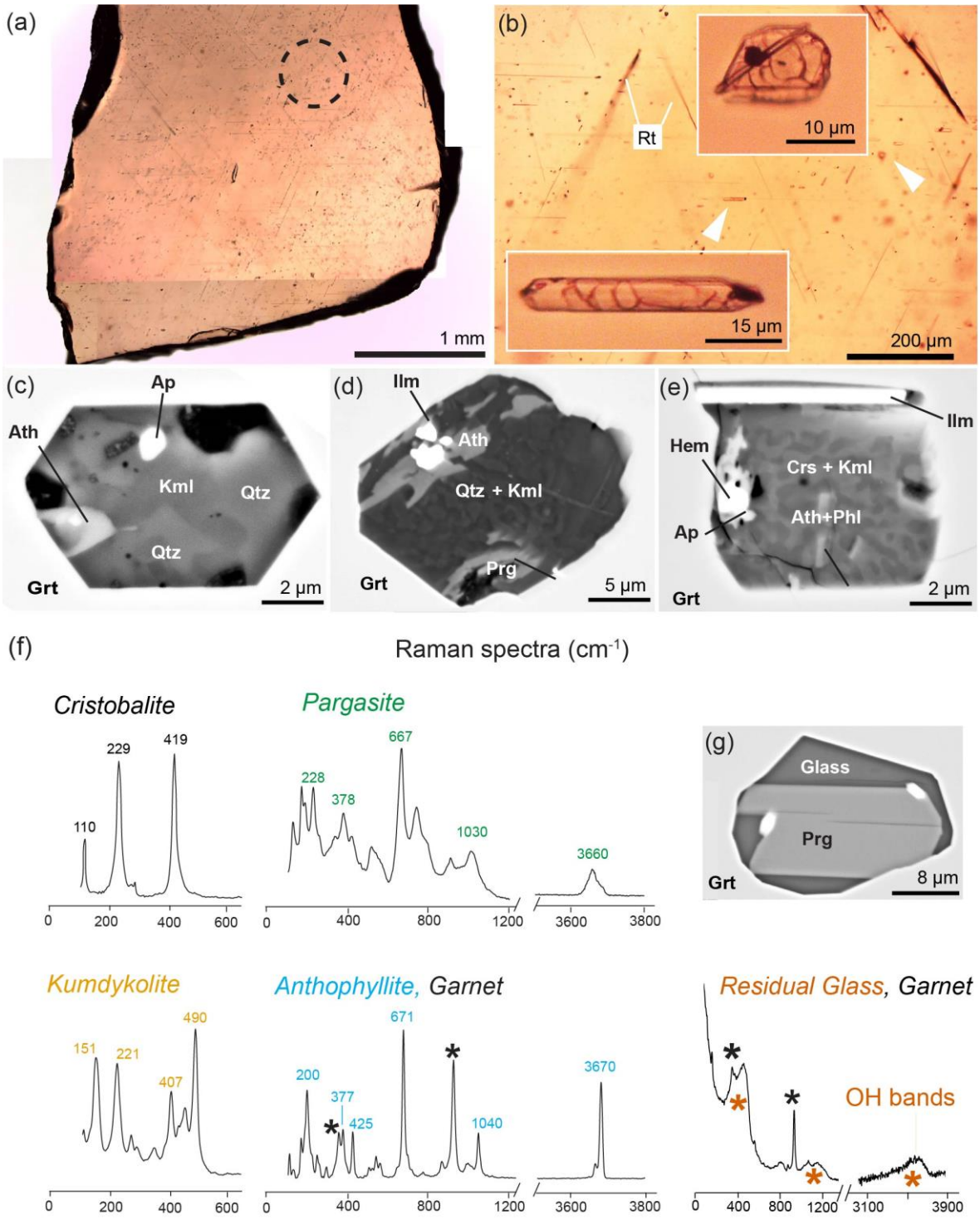

766

767 Fig. 2. Crystallized and partially crystallized melt inclusions in Gore Mountain megacrysts.
768 (a) Inclusion-bearing, doubly-polished chips of garnet megacrysts. Dashed circle=
769 location of fig. (b). (b) close up of the garnet chip with enlargements of isometric and

tubular inclusions. Rt= rutile needles. (c), (d) and (e) back scattered electron (BSE) images of the inclusions. Ath=anthophyllite, Kml=kumdykolite, Crs= Cristobalite; Qtz= quartz, Ap=apatite, Ilm=ilmenite, Prg=pargasite, Phl=phlogopite and Hem=hematite. In (d) and (e) kumdykolite and quartz/cristobalite show a typically igneous micrographic texture. (f) MicroRaman spectra of the crystalline phases in inclusions as well as glass. (g) Partially crystallized inclusion with MicroRaman spectrum of the glass visible in (f).

(a)

		Experimental runs				
Parameters	T(°C)	900	925	940	940	940	950
	P (GPa)	1.0	1.0	1.0	1.5	1.5	1.0
	t (h)	24	24	24	24	24	24
Results	Re-melting	-	Limited	+	+	+	+
	Re-hom.	-	MI <2µm	+	+	+	+
	Cracks	-	Rare	Rare	+	Rare	+
	Interaction	-	-	-	-	-	+
	Name	GM3	GM5	GM7	GM8	GM9	GM1

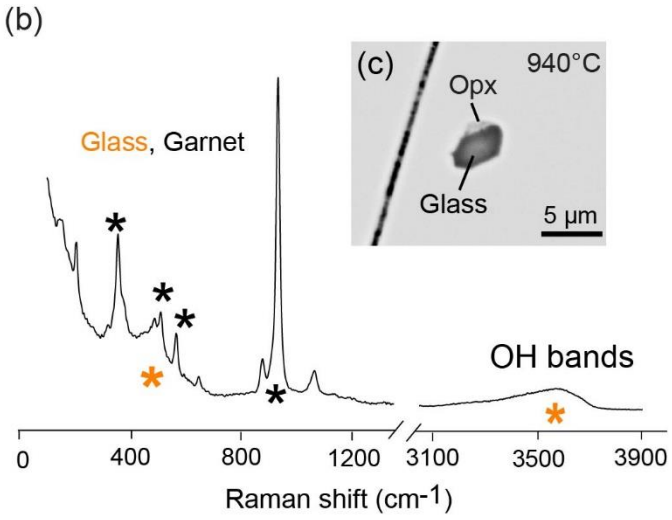

Fig. 3. Experimental re-homogenization of the inclusions. (a) Table reporting the parameters used in the re-homogenization experiments at the piston cylinder press, with relevant microstructural observations. In gray we report the two experiments where the inclusions were analyzed to obtain the composition of the original melt (Table 1). (b) Raman spectrum of the glass inside a fully re-homogenized nanogranitoid, visible in figure (c), next to an orthopyroxene interpreted as already coexisting with the melt during garnet growth and inclusion formation (see text for details).

Experiment	GM7	GM7	GM9	GM9	GM9	GM9	GM9			
No.	28	25	32-32	33	24	31	22-23	*Average*	St.Dev	Residual Glass
Trapped phases	None	Opx	Opx	Opx	Opx	Opx+Crs+Ilm	Opx			
SiO_2	69.70	71.79	75.81	73.79	72.04	72.30	67.79	*71.89*	2.06	77.58
TiO_2	0.06	0.64	0.34	0.22	0.34	0.38	0.33	*0.33*	0.19	0.01
Al_2O_3	12.93	11.36	11.46	13.43	12.52	13.57	12.82	*12.58*	0.95	12.92
FeO	3.54	4.47	2.43	4.84	3.51	2.59	2.91	*3.47*	0.97	0.80
MnO	0.04	0.00	0.07	0.12	0.07	0.01	0.01	*0.05*	0.04	0.00
MgO	1.72	2.54	0.50	1.62	1.70	1.00	0.72	*1.40*	0.70	0.06
CaO	1.80	1.38	0.92	1.78	1.72	1.52	1.55	*1.52*	0.34	0.07
Na_2O	3.02	2.21	3.49	4.22	3.86	5.55	3.86	*3.74*	1.14	4.53
K_2O	1.34	0.44	0.31	0.25	0.38	0.20	1.81	*0.67*	0.43	3.25
P_2O_5	0.02	0.20	0.07	0.00	0.00	0.10	0.03	*0.06*	0.08	0.02
Cl	0.00	0.00	0.03	0.02	0.00	0.00	0.26	*0.05*	0.01	0.00
Total	94.18	95.02	95.43	100.29	96.12	97.22	92.09	*95.77*	2.17	99.25
Q	38	48	50	38	39	33	32	*40*	7	38
C	3	5	4	3	3	2	2	*3*	1	2
Or	8	3	2	1	2	1	11	*4*	4	19
Ab	26	19	29	36	33	47	33	*32*	9	38
An	9	6	4	9	9	7	7	*7*	2	0
Hy	11	13	5	13	10	7	7	*9*	3	2
Mg#	0.46	0.50	0.26	0.37	0.46	0.41	0.30	*0.39*	0.09	0.11
ASI	1.33	1.72	1.48	1.29	1.27	1.12	1.15	*1.34*	0.21	1.16
AI	0.064	0.071	0.053	0.061	0.057	0.041	0.044	*0.06*	0.01	0.02
Na_2O/CaO	0.44	0.20	0.09	0.06	0.10	0.04	0.47	*0.20*	0.17	0.72
Al/Na+K	2.01	2.77	1.89	1.86	1.85	1.45	1.54	*1.91*	0.43	1.18
K_2O/Na_2O	1.68	1.60	3.78	2.37	2.25	3.65	2.48	*2.54*	0.87	68.0
maficity	0.09	0.13	0.05	0.11	0.09	0.06	0.06	*0.08*	0.03	0.01
H_2O by diff	5.82	4.99	4.60	-0.27	3.88	2.79	8.17	*4.28*	2.62	0.75
K#	0.23	0.12	0.06	0.04	0.06	0.02	0.24	*0.11*	0.09	0.32

Table 1. Microchemical analyses of MI and residual glass. The MI compositions were measured after experimental re-homogenization via EMP analyses. See “methods” for the alkali correction procedure. AI= Alkalinity Index (AI=molar Al-(Na+K)); maficity = total FeO and MgO contents expressed as atomic Fe + Mg; potassium number (K#) = [molar K_2O/ (K_2O + Na_2O)]. Crs= cristobalite; Opx= Orthopyroxene.

792

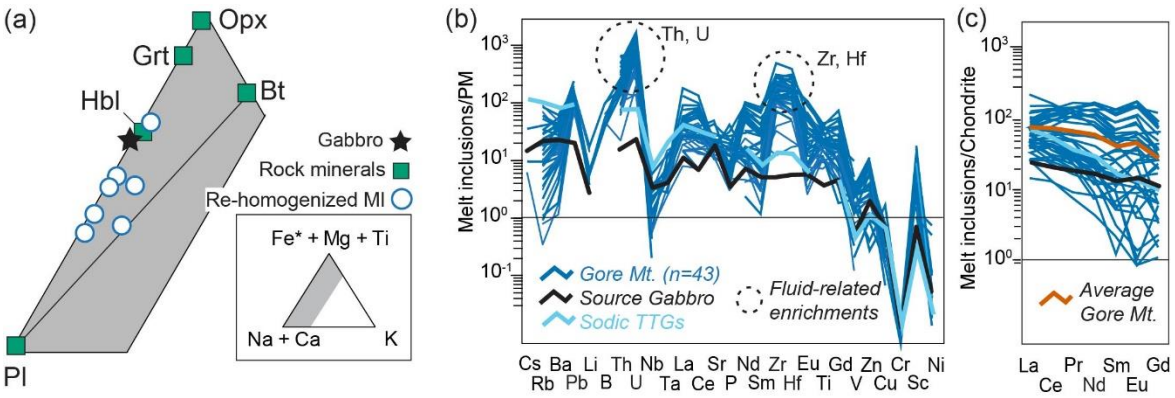

793 Fig. 4: Chemistry of the melt in inclusions. (a) Re-homogenized inclusion composition
794 versus gabbro protolith (from McLelland and Selleck, 2011) and mineral phase
795 composition in the garnet amphibolite. (b) Primitive mantle (PM)-normalized pattern of MI
796 trace elements (Table S2) versus source rock and sodic TTGs average. (c) Chondrite-
797 normalized REE patterns of MI. Y and Heavy REE (HREE) contents of the MI are not
798 available due to limitations of the deconvolution (see Methods and text). The dataset does
799 not include MI with trapped phases such as rutile, ilmenite, zircon and apatite. Sodic TTGs
800 composition is from Moyen and Martin (2012). For details on “fluid-related enrichments”
801 see section 4.4.

802

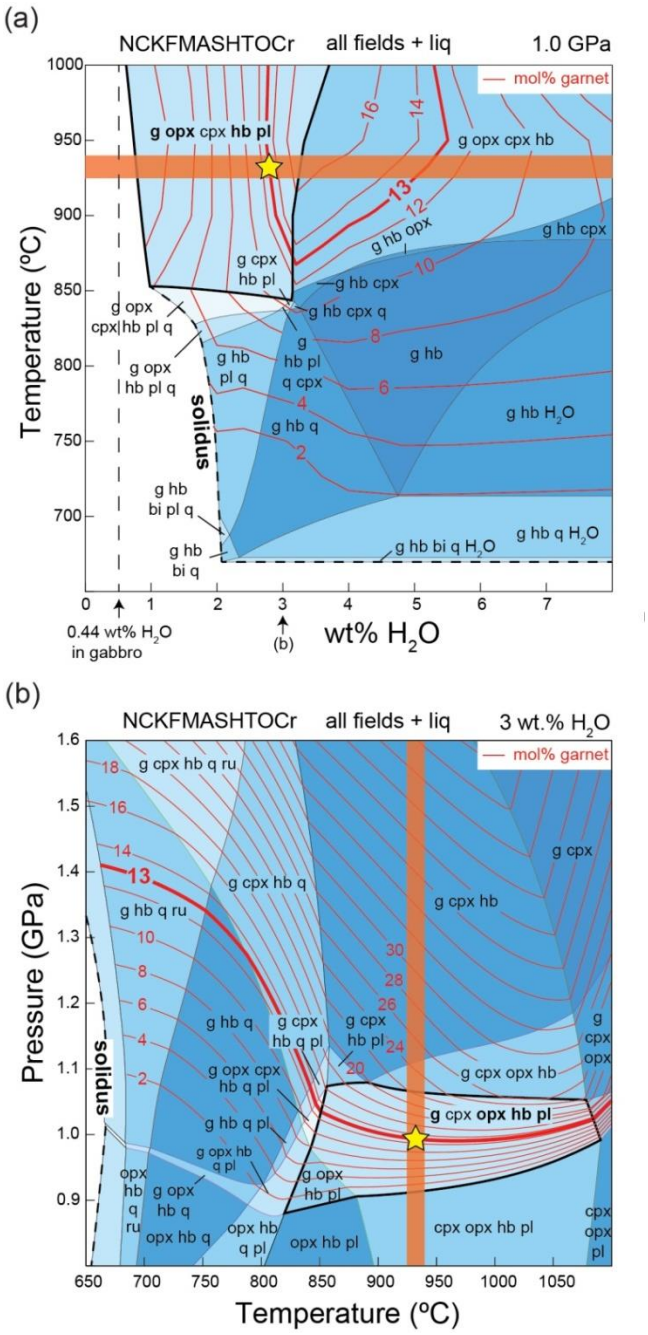

803

804 Fig. 5: Results of phase equilibrium modelling: (a) T - wt% H_2O diagram at 1.0 GPa, and
805 (b) *P-T* diagram with 3wt% H_2O, also indicated in (a). Orange box = T range at which the
806 inclusions can be successfully re-homogenized, 925-940°C. Yellow star = *PT* conditions
807 of garnet megacrysts formation as result of melting, also corresponding to melt
808 entrapment.

809 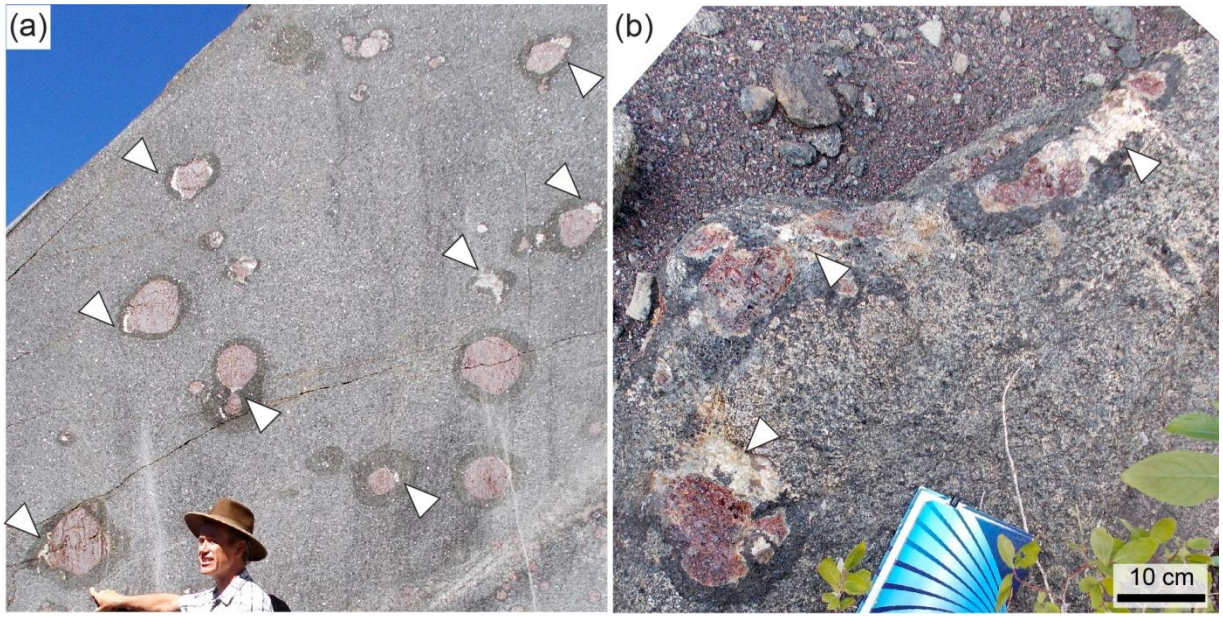

810 Fig. 6: Possible outcrop evidence for the former presence of melt. White arrows =
811 leucocratic pockets. (a) Freshly cut surface (August 2018) located in pit 3 (. (b) Loose
812 boulder in the lower part of pit 1.

813

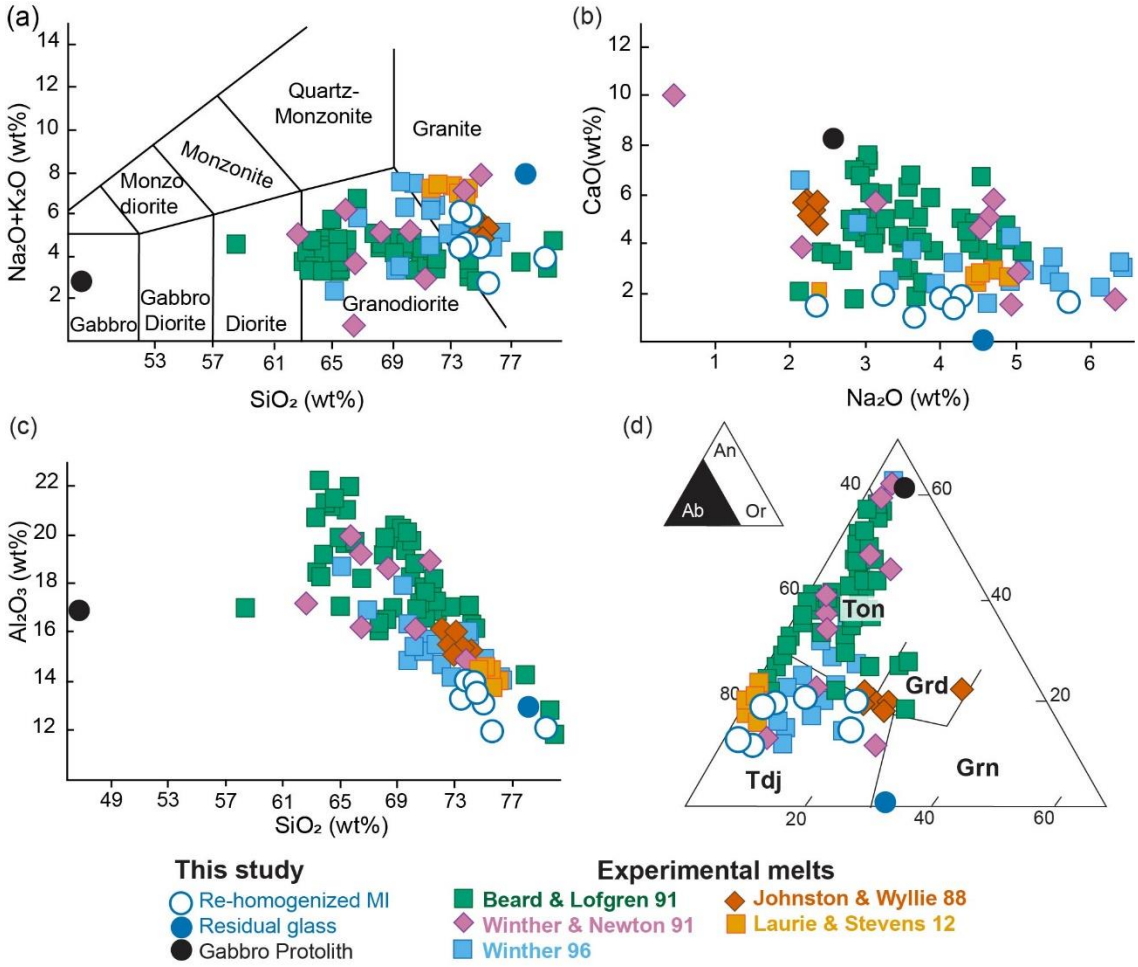

814

815 Fig. 7: Comparison between chemical features of MI from this study and melts from
816 experimental studies involving a mafic protolith re-melted in presence of H_2O. The entire
817 dataset used in the figures is visible in Supplementary file Table S3. (a) TAS diagram, (b)
818 Na_2O vs CaO plot, (c) SiO_2 vs Al_2O_3 plot and (d) Ab-Or-An ternary diagram. Tdj =
819 trondhjemite, Ton = tonalite, Grd = granodiorite and Grn = granite.

820

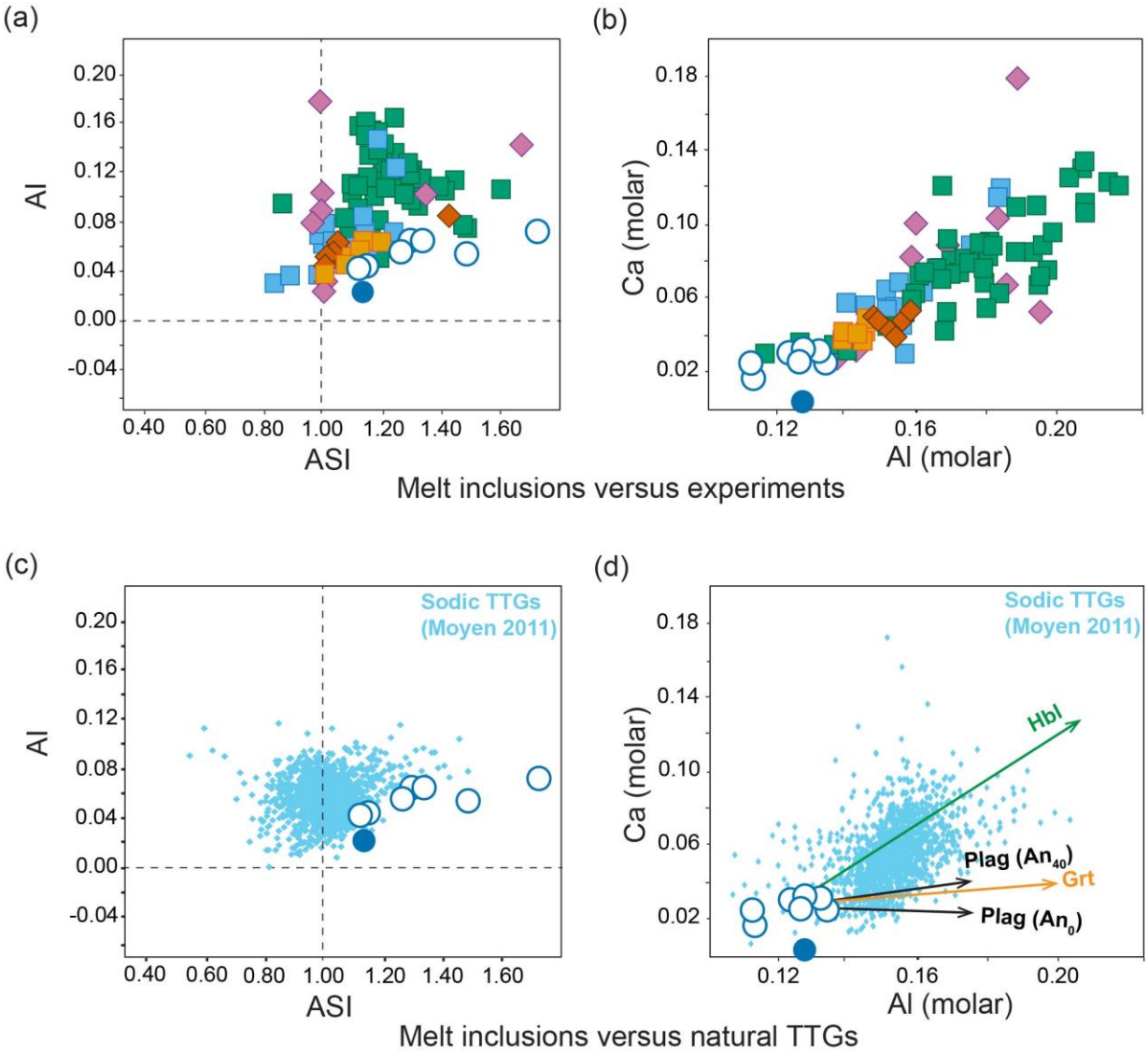

Fig. 8: ASI vs Alkalinity Index diagrams (a, c) and Molar Al vs molar Ca diagrams (b, d) of Gore Mountain MI and residual glass, experimental melts and natural TTGs. Colors for experimental melts are defined in legend Fig. 7. Enrichment vectors are visible in (d) pointing toward garnet (composition of megacrysts in Supplementary Table S1) and plagioclase and amphibole from Laurent et al. (2020).

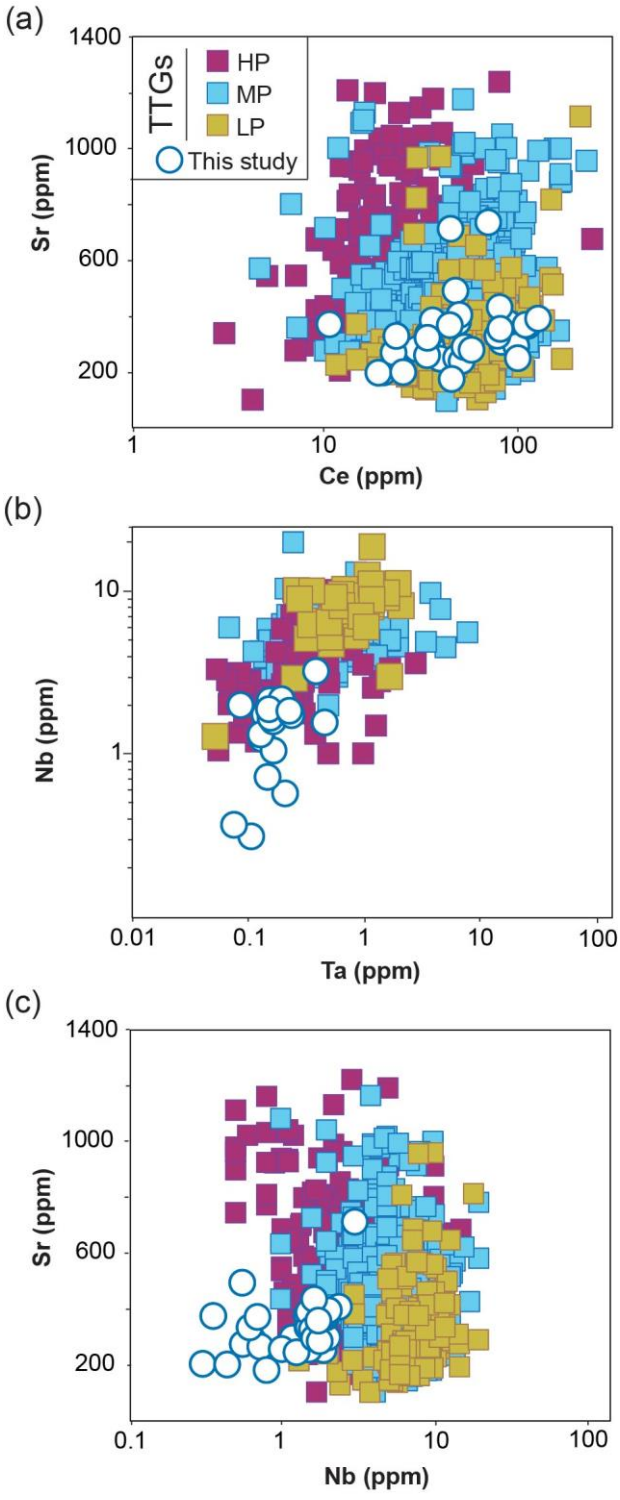

827

828 Fig. 9: Nanotrondhjemites versus TTGs. Variation diagrams of (a) Ce vs Sr, (b) Ta vs Nb

829 and (c) Nb vs Sr. Data on LP-, MP- and HP-TTGs from Moyen (2011).

Table S3

Supplementary material for online publication only

Table S3_H2O-present melting experiments from literature.xlsx

Declaration of interests

☒ The authors declare that they have no known competing financial interests or personal relationships that could have appeared to influence the work reported in this paper.

☐The authors declare the following financial interests/personal relationships which may be considered as potential competing interests:

Credit Author Statement

S.Ferrero: Conceptualization; Funding acquisition; Supervision; Interpretation; Writing - original draft; Writing - review & editing

I. Wannhoff: Investigation (microscope, microprobe analyses, imaging , Raman spectroscopy, trace element study); Methodology; Validation; Interpretation;

O.Laurent: Trace element investigation and interpretation; Interpretation; Writing

C.Yakymchuk: Investigation (Phase equilibrium modelling); Interpretation; Writing

R.S. Darling: Sampling, Interpretation; Validation

B.Wunder: Experimental Work; Interpretation

A. Borghini: Sampling; Investigation; Data reduction; Interpretation

P.J. O'Brien: Interpretation; Methodology